AMR SEMINAR #80
Ca se 1

Case contributed by: Abbas Agaimy, M.D., Erlangen, Germany.

Case history: A 22-yar-old female presented with abnormal uterine bleeding. A large uninodular uterine mass was found on clinical and imaging examination. She underwent total abdominal hysterectomy. This is a very recent case with no follow-up available.

Gross findings: The hysterectomy specimen revealed a large lobulated tan-yellow mass 9.1 cm in maximum diameter located within the myometrium with well-delineated but irregular borders to the serosal surface and the endometrium.

Histological findings: The tumor was moderately to highly cellular composed of medium-sized rounded to oval cells with rounded nuclei, variable recognizable small nucleoli and moderate rim of pale-eosinophilic to clear cytoplasm with distinct cell borders. Variable mild to moderate degrees of cytological atypia were noted from area to area. Mitoses were absent as well as coagulative necrosis. Focal plump tongue-like endovascular growth pattern, as seen in endometrial stromal sarcoma, was evident.

IHC revealed strong and diffuse cytoplasmic expression of SMA and H-caldesmon with distinct circular pericellular/ perimembranous expression of collagen IV. CD34 was diffusely positive with variable weak intensity. Desmin, CD10, ER, PR, HMB45 and ALK were negative.

Molecular testing using targeted RNA sequencing revealed an in-frame *PDGFRB::USP38* fusion.

Diagnosis: Large atypical glomus tumor of the uterus with in-frame *PDGFRB::USP38* fusion.

Discussion: Glomus tumors are uncommon mesenchymal neoplasms that display a myopericytic phenotype (recapitulate the perivascular modified smooth muscle cells of the normal glomus body). They more commonly present as small superficial nodules in the skin of the extremities (mostly acral or subungual) and less frequently as much larger masses in deep soft tissue and in the viscera including the gastrointestinal tract, the genitourinary system, the mediastinum, bones and the lungs. Among visceral locations, the stomach represents the most frequently affected site.

Syndromic glomus tumors have been reported in the setting of the multiple familial glomus tumor syndrome (glomuvenous malformations), an autosomal dominant disease characterized by multiple glomus tumors/glomuvenous malformations because of germline mutations in the glomulin gene (*GLMN*), and in neurofibromatosis type 1. Otherwise, no predisposing risk factors have been identified.

At a molecular level, most sporadic malignant glomus tumors have been found to harbor *NOTCH* gene family rearrangements (mostly *NOTCH2*). *BRAF* mutations have been associated with malignant histology in glomus tumors lacking *NOTCH* gene alterations. In the appropriate morphological context, immunohistochemical demonstration of SMA and pericellular collagen IV expression is diagnostic.

The current case did not fulfil the minimal criteria for malignant glomus tumor (either marked nuclear atypia with any mitotic activity or atypical mitotic figures). Other atypical features such as spindled morphology and infiltrative growth pattern were absent. The tumor, however, is large and deeply located, hence should be considered a glomus tumor of uncertain malignant potential.

The literature on glomus tumors of the GYN tract is sparse. A quick search of the MEDLINE literature disclosed a mention of uterine glomus tumor dating back to 1958 (by Borghard-Erdle and Hirsch). An incidental (2mm) microscopic glomus tumor of the uterine cervix was reported by Aynardi et al in 2016, who cited two prior similar cases. It is however possible or even likely that larger tumors have been mistaken for epithelioid leiomyomatous neoplasms. The *PDGFRB* fusion detected herein is potentially of therapeutic relevance using tyrosine kinase inhibitors. However, this exact fusion (with USP38 as fusion partner) is novel and has not been reported before.

The differential of the current case depends on the type of the examined specimen (small curettage biopsies vs resection) and encompasses epithelioid smooth muscle tumors, low-grade endometrial stroma sarcoma, PEComas, plexiform uterine tumorlets and others.

This case should contribute to alerting members of the club to include this rare tumor in the differential of epithelioid mesenchymal neoplasms of the uterus.

References:

- Borghard-Erdle AM, Hirsch EF. Glomus tumor of the uterus. AMA Arch Pathol. 1958 Mar;65(3):244-6.
- Aynardi JT, Kim SH, Barroeta JE. Epithelioid Glomus Tumor of the Uterine Cervix: A Case Report and Review. Int J Gynecol Pathol. 2016 May;35(3):275-8.
- Nunez-Alonso C, Battifora HA. Plexiform tumors of the uterus: ultrastructural study. Cancer. 1979 Nov;44(5):1707-14. doi: 10.1002/1097-0142(197911)44:5<1707::aid-cncr2820440526>3.0.co;2-5.
- Sakai Y. Epithelioid vascular leiomyoma of the uterus mimicking glomangiomyoma. Arch Gynecol Obstet. 2007 Jan;275(1):59-61.
- Van Geertruyden J, Lorea P, Goldschmidt D, et al. Glomus tumours of the hand. A retrospective study of 51 cases. J Hand Surg Br. 1996 Apr;21(2):257-60.
- Boon LM, Brouillard P, Irrthum A, et al. A gene for inherited cutaneous venous anomalies ("glomangiomas") localizes to chromosome 1p21-22. Am J Hum Genet. 1999 Jul;65(1):125-33.

- Brouillard P, Boon LM, Mulliken JB, et al. Mutations in a novel factor, glomulin, are responsible for glomuvenous malformations ("glomangiomas"). Am J Hum Genet. 2002 Apr;70(4):866-74.
- Gaertner EM, Steinberg DM, Huber M, et al. Pulmonary and mediastinal glomus tumors--report of five cases including a pulmonary glomangiosarcoma: a clinicopathologic study with literature review. Am J Surg Pathol. 2000 Aug;24(8):1105-14.
- Folpe AL, Fanburg-Smith JC, Miettinen M, et al. Atypical and malignant glomus tumors: analysis of 52 cases, with a proposal for the reclassification of glomus tumors. Am J Surg Pathol. 2001 Jan;25(1):1-12.
- Miettinen M, Paal E, Lasota J, et al. Gastrointestinal glomus tumors: a clinicopathologic, immunohistochemical, and molecular genetic study of 32 cases. Am J Surg Pathol. 2002 Mar;26(3):301-11.
- De Smet L, Sciot R, Legius E. Multifocal glomus tumours of the fingers in two patients with neurofibromatosis type 1. J Med Genet. 2002 Aug;39(8):e45.
- Brems H, Park C, Maertens O, et al. Glomus tumors in neurofibromatosis type 1: genetic, functional, and clinical evidence of a novel association. Cancer Res. 2009 Sep;69(18):7393-401.
- Shim HS, Choi YD, Cho NH. Malignant glomus tumor of the urinary bladder. Arch Pathol Lab Med. 2005 Jul;129(7):940-2.
- Masson-Lecomte A, Rocher L, Ferlicot S, et al. High-flow priapism due to a malignant glomus tumor (glomangiosarcoma) of the corpus cavernosum. J Sex Med. 2011 Dec;8(12):3518-22.
- Chakrapani A, Warrick A, Nelson D, et al. BRAF and KRAS mutations in sporadic glomus tumors. Am J Dermatopathol. 2012 Jul;34(5):533-5.
- Mosquera JM, Sboner A, Zhang L, et al. Novel MIR143-NOTCH fusions in benign and malignant glomus tumors. Genes Chromosomes Cancer. 2013 Nov;52(11):1075-87.
- Mravic M, LaChaud G, Nguyen A, et al. Clinical and histopathological diagnosis of glomus tumor: an institutional experience of 138 cases. Int J Surg Pathol. 2015 May;23(3):181-8.
- Sirohi D, Smith SC, Epstein JI, et al. Pericytic tumors of the kidney-a clinicopathologic analysis of 17 cases. Hum Pathol. 2017 Jun;64:106-117.
- Karamzadeh Dashti N, Bahrami A, Lee SJ, et al. BRAF V600E Mutations Occur in a Subset of Glomus Tumors, and are Associated With Malignant Histologic Characteristics. Am J Surg Pathol. 2017 Nov;41(11):1532-1541.

AMR SEMINAR #80
Ca se 2

Case contributed by: Reza Alahghebandan, M.D., Cleveland Clinic, USA.

Case History
A 54-year-old man presented with an adrenal mass. Imaging revealed 6.5 cm adrenal mass with multiple solid pulmonary masses.

Gross findings
A well-circumscribed 6.5 x 4.5 x 3.7 cm tan-gray fleshy mass with central hemorrhagic/necrotic area (30%).

Microscopic findings
Histologic sections show an undifferentiated malignant neoplasm in solid growth pattern composed of neoplastic cells with high-grade morphology, rhabdoid features, associated with frequent mitoses, apoptosis and extensive necrosis. At the periphery, there is a rim of

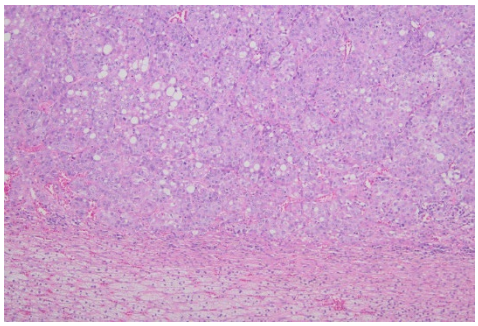
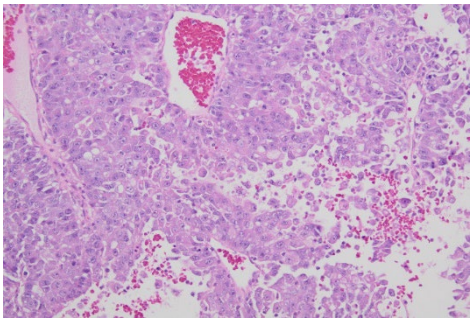
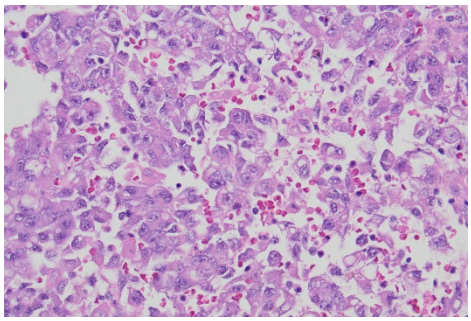

unremarkable renal cortical tissue present.

Immunohistochemical stains show the neoplastic cells to be positive for CAM 5.2 and CK7, while being negative for CK20, SF1, PAX8, GATA3, CDX2, NKX3.1, TTF-1, CD20, and CD3. Ki-67 shows a proliferation index of approximately 90%. Further stains show the neoplastic cells to have retained INI1 and SMARCA2 pattern, while showing loss of SMARCA4.

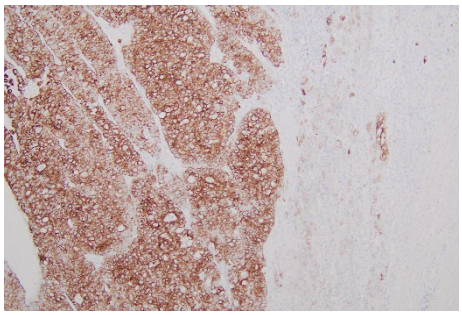
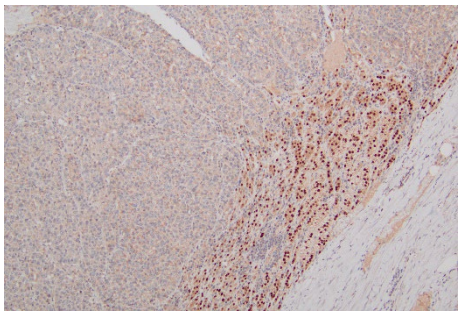
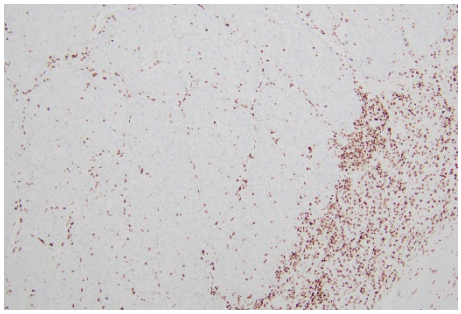

CAM5.2 **SF1** **SMARCA4**

Diagnosis: SMARCA4-deficient undifferentiated carcinoma.

Comments: There has certainly been an evolution in the SWI/SNF family of tumors (mainly SMARCA4 and B1) over the last decade. These tumors are clinically aggressive, with a rhabdoid morphology, recognized in various anatomic locations with different terminologies (sarcoma, carcinoma, tumors, etc).

In this case, my main differential diagnosis included a primary adrenocortical carcinoma versus metastasis (i.e., carcinoma, melanoma, etc). Although SF-1 was negative in this tumor, one might argue for the possibility of primary adrenal SMARCA4-deficient undifferentiated tumor. However, we know that comprehensive genomic characterization of adrenocortical carcinomas has not revealed SMARCA4 alterations. Further, there is no documented association between adrenocortical carcinoma and SMARCA4-undifferentiated component. This patient also presented with multiple lung masses, which is consistent with the literature that SMARCA4-deficient undifferentiated tumors may present as dominant adrenal masses and likely represent metastases from thoracic primaries.

And finally, I signed this case out as an undifferentiated "carcinoma" given strong keratin staining and more importantly preventing confusion for the care team. The patient has been treated with immune checkpoint inhibitor, alive with no progression 6 months post-therapy. Generally, cytotoxic chemotherapy regimens are ineffective in these tumors.

Selected references

- Ashour S, Reynolds JP, Mukhopadhyay S, McKenney JK. SMARCA4-Deficient Undifferentiated Tumor Diagnosed on Adrenal Sampling. Am J Clin Pathol. 2022 Jan 6;157(1):140-145.
- Agaimy A. SWI/SNF Complex-Deficient Soft Tissue Neoplasms: A Pattern-Based Approach to Diagnosis and Differential Diagnosis. Surg Pathol Clin. 2019 Mar;12(1):149-163.
- Schaefer IM, Hornick JL. SWI/SNF complex-deficient soft tissue neoplasms: An update. Semin Diagn Pathol. 2021 May;38(3):222-231.
- Agaimy A, Bertz S, Cheng L, Hes O, Junker K, Keck B, Lopez-Beltran A, Stöckle M, Wullich B, Hartmann A. Loss of expression of the SWI/SNF complex is a frequent event in undifferentiated/dedifferentiated urothelial carcinoma of the urinary tract. Virchows Arch. 2016 Sep;469(3):321-30.
- Agaimy A, Cheng L, Egevad L, Feyerabend B, Hes O, Keck B, Pizzolitto S, Sioletic S, Wullich B, Hartmann A. Rhabdoid and Undifferentiated Phenotype in Renal Cell Carcinoma: Analysis of 32 Cases Indicating a Distinctive Common Pathway of Dedifferentiation Frequently Associated With SWI/SNF Complex Deficiency. Am J Surg Pathol. 2017 Feb;41(2):253-262.
- Agaimy A, Jain D, Uddin N, Rooper LM, Bishop JA. SMARCA4-deficient Sinonasal Carcinoma: A Series of 10 Cases Expanding the Genetic Spectrum of SWI/SNF-driven Sinonasal Malignancies. Am J Surg Pathol. 2020 May;44(5):703-710.
- Agaimy A, Thiel F, Hartmann A, Fukunaga M. SMARCA4-deficient undifferentiated carcinoma of the ovary (small cell carcinoma, hypercalcemic type): clinicopathologic and immunohistochemical study of 3 cases. Ann Diagn Pathol. 2015 Oct;19(5):283-7.

- Zheng S, Cherniack AD, Dewal N, Moffitt RA, Danilova L, Murray BA, Lerario AM, Else T, Knijnenburg TA, Ciriello G, Kim S, Assie G, Morozova O, Akbani R, Shih J, Hoadley KA, Choueiri TK, Waldmann J, Mete O, Robertson AG, Wu HT, Raphael BJ, Shao L, Meyerson M, Demeure MJ, Beuschlein F, Gill AJ, Sidhu SB, Almeida MQ, Fragoso MCBV, Cope LM, Kebebew E, Habra MA, Whitsett TG, Bussey KJ, Rainey WE, Asa SL, Bertherat J, Fassnacht M, Wheeler DA; Cancer Genome Atlas Research Network; Hammer GD, Giordano TJ, Verhaak RGW. Comprehensive Pan-Genomic Characterization of Adrenocortical Carcinoma. Cancer Cell. 2016 Aug 8;30(2):363. doi: 10.1016/j.ccell.2016.07.013. Epub 2016 Aug 8. Erratum for: Cancer Cell. 2016 May 9;29(5):723-736.

AMR SEMINAR #80
Ca se 3

Case contributed by: Gerald Berry, M.D., Stanford University, USA.

Clinical History: A previously healthy 19-year-old woman presented with cardiac cachexia (a 30-lb weight loss over a 6 month period of time), along with progressive dyspnea on exertion and weakness. A systolic ejection murmur was heard on physical examination together with mild peripheral edema in the lower extremities. Echocardiography showed an interventricular mass causing LV outflow tract obstruction. CT angiography showed a 6.0 x 4.4 x 3.8 cm mass (Figure 1) that was mildly hypermetabolic on PET scan. Multiple attempts at a tissue diagnosis by endomyocardial biopsy were undertaken without success. These included 1. Via right atrium, 2. Via right ventricle, 3. Via aortic valve and left ventricle, 4. Transeptal through the MV. An intraoperative Tru-Cut needle biopsy was performed and the diagnosis of hamartoma of mature cardiac myocytes was made. She underwent tumor debulking and concomitant aortic valve replacement and mitral valve repair with placement of a mitral ring. The patient quickly recovered and within a few months was gaining weight and was free of any dyspnea symptoms.

Pathologic Findings: Both the Tru-Cut needle and the subsequent tumor debulking specimen showed similar findings. (The provided slide is from the resection specimen) The edge of the unencapsulated lesion showed a sharp demarcation from the normal myocardium. The mass was composed of enlarged, irregularly distributed and disorganized myocytes with bands of dense collagenous fibrosis containing dilated venules and adipose tissue. The branching thick-walled vessels of hemangioma were absent.

Diagnosis: Hamartoma of mature cardiac myocytes.

Discussion: This lesion is uncommon with around 100 cases now reported in the literature. They show a male predilection (2:1) and can present across a wide age spectrum (infancy to geriatrics) with a mean around 25 years of age. In the AFIP series of 15 cases, 6 were located in the LV, 3 in the RA and 2 each in the IVS or RV or in multiple sites. The mean size was 5.0cm ranging from microscopic (usually an incidental finding) up to 9.0 cm. As in this case, they often appear poorly circumscribed and can be challenging for the surgeon to determine adequate surgical margins. Microscopically, the marked disarray alignment of myocytes together with the fibrosis and fat are characteristic. Myocyte vacuolization has been described but is limited (unlike a rhabdomyoma (a hamartoma of infants and children). The presentation as a mass distinguishes it from hypertrophic cardiomyopathy.

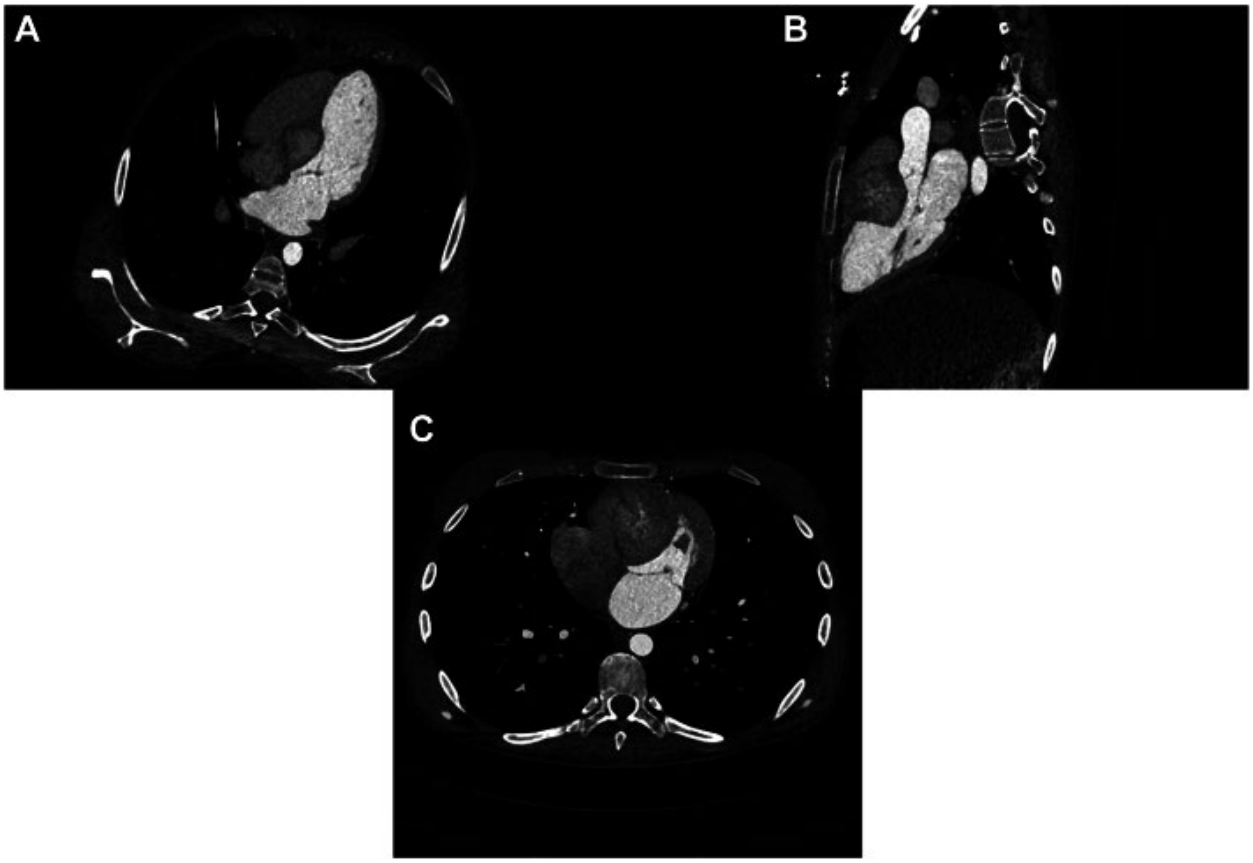

Figure 1: CT image of the IVS mass: A- 4-chamber view; B- left ventricular long axis, C- short-axis view.

References:

- Sturtz CL et al. Mod Pathol 1998; 11:496-99.
- Fealey ME et al. Hum Pathol 2008; 39:1064-71.
- Burke AP, et al. Hum Pathol 1998; 29:904-09.

AMR SEMINAR #80
Ca se 4

Case contributed by: Ira Bleiweiss, M.D., University of Pennsylvania, USA.

Clinical history: A 61 year old male presented with a palpable right breast mass. He had a past medical history of 2 prior left partial nephrectomies for clear cell carcinoma (6 and 12 years ago). Family history: Mother: Breast cancer in her 40's, Sister: Breast cancer in her 60's, Sister: Ovarian cancer, Father: prostate cancer.

Mammogram (below left): Right breast 1:00, retroareolar well circumscribed mass

Ultrasound (below right): 1 cm from nipple, oval, heterogenous, solid mass 1.2x1.1x0.7 cm

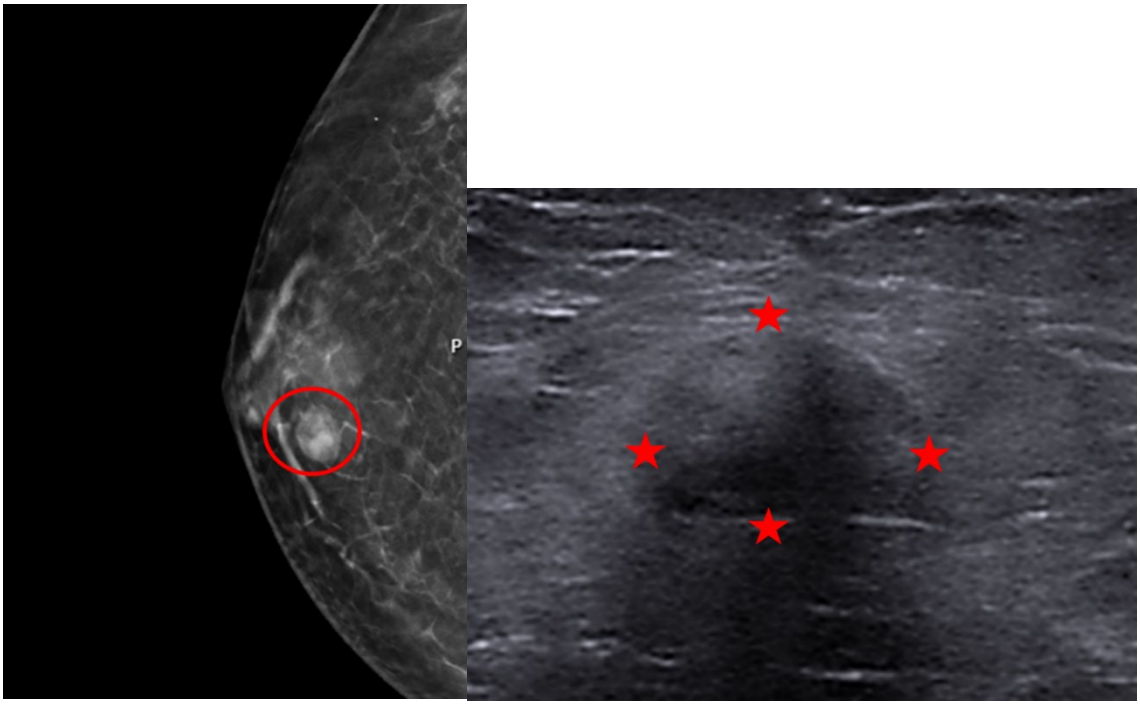

The lesion was biopsied (below), correctly diagnosed, and then excised. The slides submitted are from the excision.

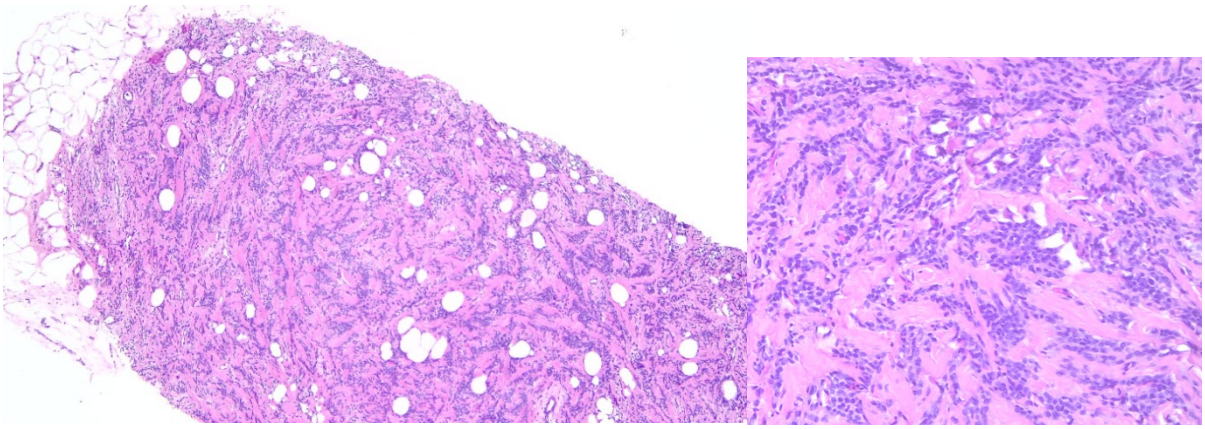

Pathologic Findings: Well circumscribed mass of bland spindle cells arranged in short haphazard intersecting fascicles in between areas of keloid-like eosinophilic collagen and variable amounts of fat. Focally the cells are more epithelioid. IHC: + for CD34, - for keratins

Diagnosis: Myofibroblastoma with focal epithelioid features (and biopsy site).

Comment: I thought for a change I would send a classic, no frills, non-controversial case which would be nice for everyone's teaching files. This is a classic myofibroblastoma. In the older literature this lesion was a male-predominant mass, of course presenting as a palpable lesion. With the advent of routine mammographic screening, women have caught up and probably overtaken the men! The most important thing to remember about these benign tumors is that they are well-circumscribed round to oval lesions. I have seen several cases (in both men and women) in which the cells become very epithelioid and even have atypia (but no mitoses) and may be a dead ringer for invasive lobular carcinoma. One will not fall into this trap if one remembers that invasive lobular carcinoma does not present as a well circumscribed round to oval mass. In such a situation, it is important to do keratin stains since myofibroblastoma can be positive for estrogen and progesterone receptors, and therefore they can be misleading. In my experience these are always benign, although I recall one case many years ago of a spindle cell sarcomatous breast lesion that in areas resembled the pattern of myofibroblastoma albeit entirely composed of cytologically malignant cells.

AMR SEMINAR #80
Ca se 5

Case contributed by: Alberto Cavazza, M.D., Reggio-Emilia, Italy.

Clinical presentation and histology. A 31 year old woman underwent a right pulmonary apicectomy due to recurrent pneumothorax. Together with the typical histologic features of pneumothorax (pleuritis, mild subpleural fibrosis), the biopsy shows some small intraparenchymal cysts, consisting in discrete, rounded, mainly paraseptal dilatations of the alveolar spaces, sometimes with a back-to-back configuration sometimes with a back-to-back configuration (please refer to the figure below, because the most significant lesions are focal and in some of your slides are not well represented). The surrounding lung parenchyma is unremarkable.

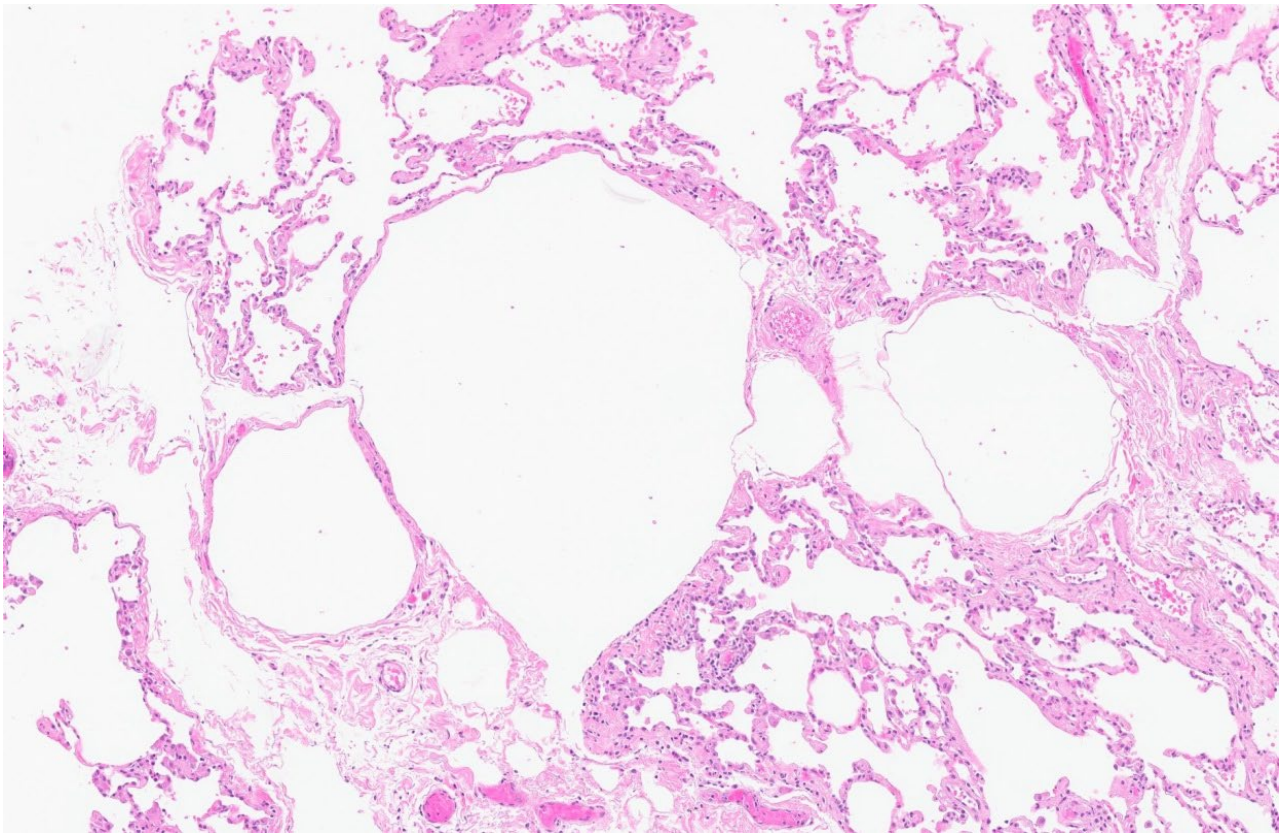

Diagnosis. I did a descriptive report and suggested to evaluate the possibility of Birt-Hogg-Dubé (BHD) syndrome, which was confirmed genetically.

Comments. Pneumothorax is a relatively common condition, in which air penetrates the pleural cavity. It can be divided into primary and secondary: the latter is less frequent and occurs from a variety of diseases. Patients are generally treated conservatively, and surgical specimens are

obtained infrequently: when we receive these specimens, our goal is to recognize an underlying significant disease, particularly If clinically unexpected.

Primary (spontaneous) pneumothorax usually occurs in young, thin men, particularly smokers: outside this clinical setting, the possibility of an underlying disease causing pneumothorax increases. Primary pneumothorax is presumed to be due from rupture of intrapleural blebs or subpleural bullae. At histology, apart blebs and bullae, a variety of nonspecific findings can be found including pleuritis, subpleural fibrosis sometimes with fibroblastic foci, inflammation sometimes with many eosinophils (which may involve the vascular walls simulating vasculitis), pleural/subpleural vascular wall thickening and vascular proliferation (sometimes so prominent to simulate a vascular malformation), subpleural foci of acute lung injury with pneumocyte hyperplasia, and giant cells surrounding persistent interstitial air. These findings are secondary to pneumothorax, and none of them have clinical significance in this setting. Underlying smoking changes, particularly finely pigmented smoker's macrophages, are frequent as well.

Secondary pneumothorax can be due to many different diseases, both neoplastic and non-neoplastic. Among the latter, endometriosis and cystic lung diseases can be particularly subtle at histology. The main diseases presenting as cysts in the lung are lymphangioleiomyomatosis, Langerhans cell histiocytosis and BHD syndrome. The latter is a rare, autosomal-dominant systemic disorder due to defect of a gene which encodes folliculin, a protein involved in multiple signaling pathways. Clinically, BHD has an equal sex distribution and is characterized by a variable combination of cutaneous lesions (mostly fibrofolliculomas, presenting as small papules in the head/neck and upper trunk), a variety of kidney tumors and pneumothorax due to lung cysts. At CT of the chest, the cysts of BHD prevail in the lower lobes and vary in dimension and shape. At histology, they tend to abut on interlobular septa, sometimes with venules protruding into the lumen, and with intracystic septa creating a back-to-back appearance. The inner surface of the cysts is lined by a layer of flat pneumocytes, and the wall is thin, without significant inflammation or fibrosis. The surrounding lung is generally preserved, unlike emphysema in which a background of smoking-related changes is frequently present. These histologic findings are not pathognomonic, but they are sufficiently characteristic to allow the pathologist to suggest the possibility of BHD syndrome: the diagnosis requires genetic confirmation; however our suggestion is important because of the risk of these patients to develop carcinomas in different organs, particularly the kidneys.

References.

- Schneider F et al. Approach to lung biopsies from patients with pneumothorax. Arch Pathol Lab Med 2014;138:257-265.

- Johnson SR et al. Diagnosis of cystic lung diseases: a position statement from the UK cystic lung disease rare disease collaborative network. Thorax 2024;79:366-377.

- Furuya et al. Pathology of Birt-Hogg-Dubé syndrome: a special reference of pulmonary manifestations in a Japanese population with a comprehensive analysis and review. Pathol Intern 2019;69:1-12.

AMR SEMINAR #80
Ca se 6

Case contributed by: Kum Cooper, M.D., University of Pennsylvania, USA.

Case History: 56 years old woman with 4cm parapharyngeal mass, resected (sections submitted). Was followed by lymph node neck dissection a few weeks later.

Diagnosis: Follicular dendritic cell sarcoma (FDCS) in the setting of Castleman's disease.

Comment: The diagnosis was confirmed with CD21, CD23 and CD35. Other relevant lymphoid markers were non-contributory. Adjacent to the tumor (as seen in your section), features of a unicentric hyaline-vascular type Castleman disease (HV-CD) with FDC expansion is present. In some of the "lollipop" follicles dysplastic FDC are also identified.

These features were first described by John Chan in the late nineties and proposed to be the precursors to FDCS in the setting of HV-CD. Interestingly (sections not submitted), unicentric-type CD was present in two of the level 2 lymph nodes. So, in fact, this is an FDCS arising in a multicentric HV-CD.

I was not aware of the latter concept and found an abstract in Blood (reference below) referring to this as a "missing link". Blood 142 (2023) 2033-2034.

AMR SEMINAR #80
Ca se 7

Case contributed by: Goran Elmberger, M.D., Linköping, Sweden.

Case History: A 67-year-old female with a history of smoking and alcohol abuse presented with complaints of unilateral left-sided nasal obstruction. Clinical examination revealed a large unilateral intranasal tumor. Computed tomography (CT) showed a mass filling the left nasal cavity with destruction of the nasal septum, orbital wall, and sinus walls, and suspicious involvement of the overlying skin. Magnetic resonance imaging (MRI) identified an expansile mass measuring 6 x 4 x 2 cm, with destruction of the nasal septum and the medial wall of the maxillary sinus. The radiological findings were suspicious for malignancy, with a staging of rT2(3)N0M0. There was a clinical and radiological concern for **s**inonasal carcinoma or lymphoma.

Pathological Findings: Initial biopsies from an external hospital were reviewed by our soft tissue pathology team. The samples were described as a vascular lesion with a complex anastomosing pattern and mild to moderate endothelial nuclear atypia. Immunohistochemical staining indicated a vascular lesion, with positive results for endothelial markers CD31, CD34, and ERG, and negative results for D2-40. Smooth muscle actin (SMA) was positive in a continuous pericyte layer. The Ki-67 index was low at 5%. In the initial report, concerns were raised regarding the possibility of a low-grade angiosarcoma due to the clinical and radiological suspicion of malignancy, the tumor's clinical and radiological destructive growth, and its large size. A phenomenon described in dermatopathology as "deceptively bland cutaneous angiosarcoma on the nose mimicking hemangioma" was also mentioned. Ultimately, the lesion was classified as an atypical vascular proliferation suspicious for angiosarcoma. A resection was performed following embolization due to the suspicion of angiosarcoma. The specimen, measuring 3.5 x 2.5 x 1.0 cm was sent in formalin to our sarcoma team.

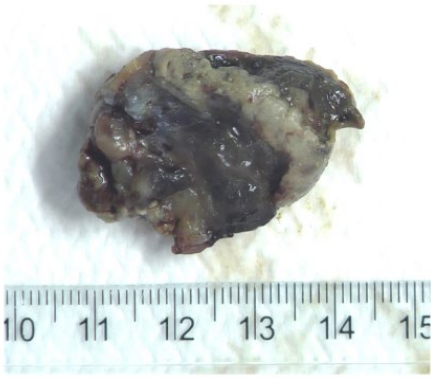

Following extensive immunohistochemistry, the final diagnosis was determined to be uncertain but most likely a hemangioma variant, with no evidence of malignancy.

I first encountered the case while preparing for our ENT multidisciplinary conference. My impression was that of an antrochoanal polyp (ACP) with severe angioproliferation, likely reactive and secondary to ischemic changes. At low magnification, a polyp with epithelial coverage on three surfaces was observed. The lesion was lined by respiratory epithelium, metaplastic squamous epithelium, and areas with surface erosions. Pseudoepitheliomatous hyperplasia (PEH) and sialometaplasia were noted focally within the squamous epithelium. Following embolization, hemorrhage and infarction were prominent; however, the basic pathology matched the findings in previous biopsies. The most striking feature was a lobular proliferation of capillary vessels, with some larger central "feeding" vessels, partially arteriolar in nature. Mild nuclear atypia in the endothelial cells was observed, likely representing reactive hyperplasia. The stroma was fibrotic and reactive, with abundant hemosiderin pigment. Slightly atypical stromal myofibroblasts (ASCs) were also noted. Otherwise, the lesion resembled typical sinonasal polyps, except for the relative absence of mucous glands and eosinophilic inflammatory infiltrates. Central regions of the lesion showed minimal inflammation. Features of recent embolization included hyperemia, hemorrhage, and zonal necrosis.

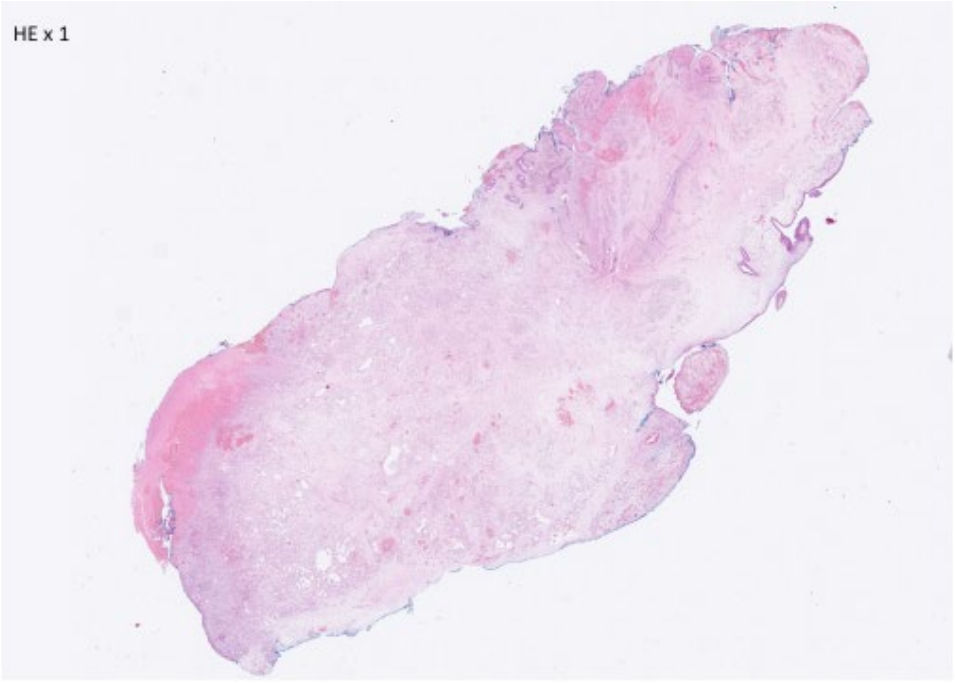

Immunohistochemical analysis revealed that ASCs were positive for vimentin and SMA, while pancytokeratin was negative. Desmin, myogenin, CD31, CD34, MyoD1, and ALK1 were negative.

□□

The vascular structures were positive for CD31, CD34, and ERG, with negative D2-40. A continuous layer of SMA-positive pericytes surrounded the vessels.

The Ki-67 index was low, at 2-3%.

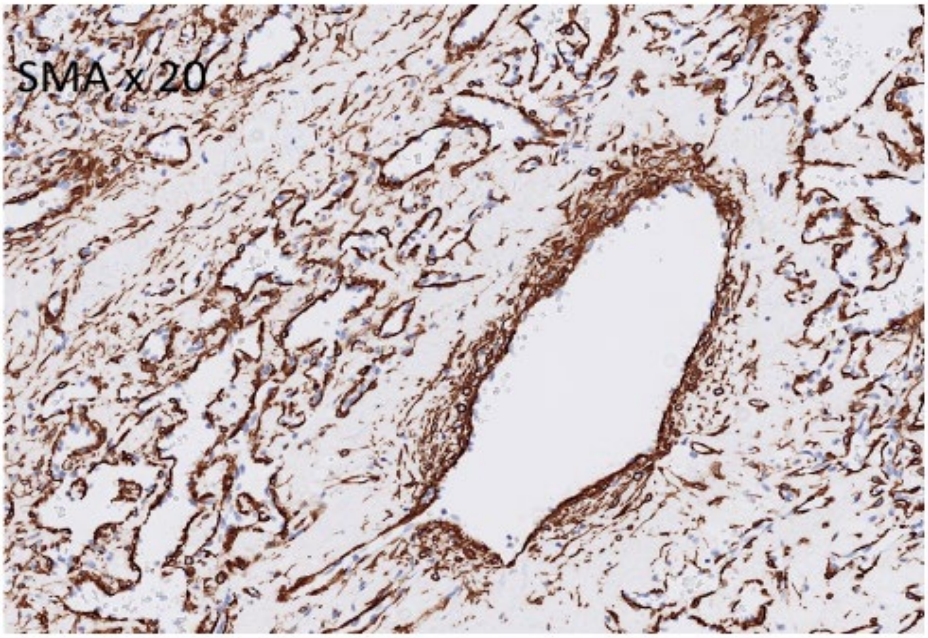

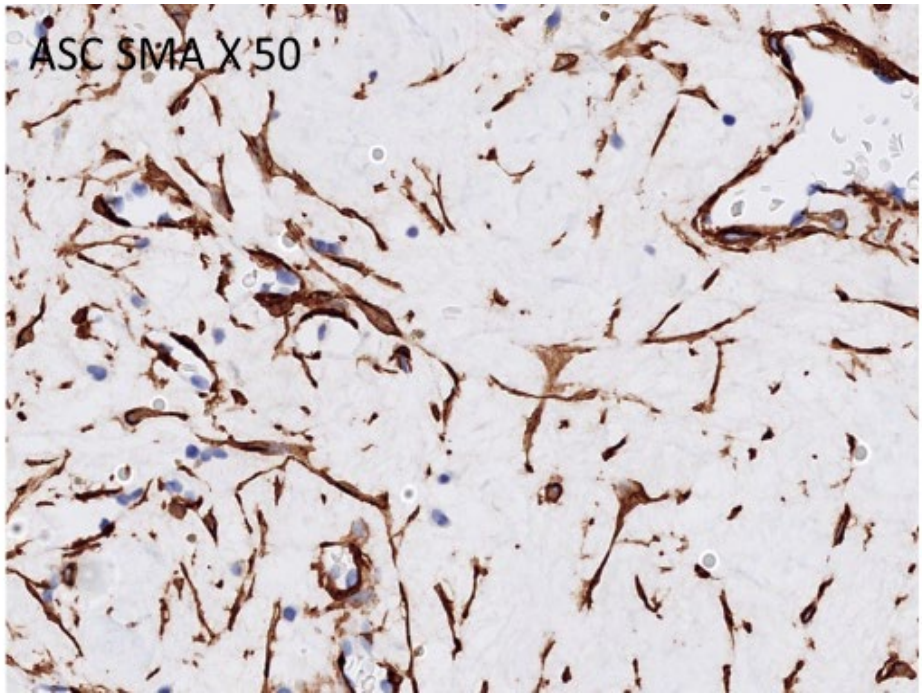

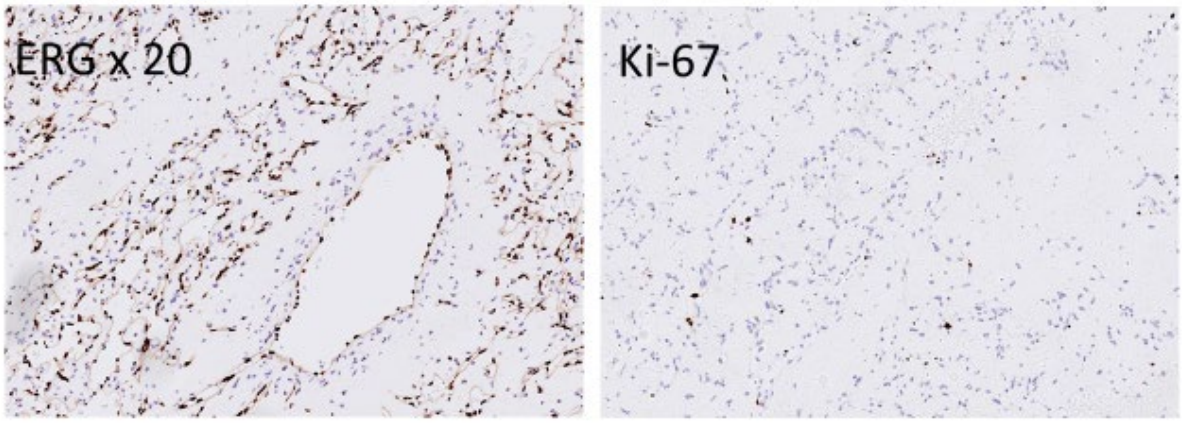

Diagnosis: Angiomatous Antrochoanal Polyp (ACP).

Follow-up: The patient experienced no further complications following resection, with a follow-up duration of two months.

Discussion: Antrochoanal polyps (ACPs) are benign, large inflammatory polyps that originate within the maxillary sinus and extend through the natural or accessory ostium into the nasal cavity, often reaching the choana. ACPs are relatively rare, accounting for 3%-6% of all nasal polyps. Histologically, ACPs demonstrate greater inflammatory cell infiltration and less eosinophilic infiltration and submucosal glands compared to typical inflammatory nasal polyps. This suggests that ACPs are more closely associated with underlying inflammatory processes rather than allergic reactions.

Diagnosis is primarily clinical, supported by radiological imaging, typically, CT scans. However, radiological signs of bony destruction can be present in both benign expansile and malignant destructive lesions. At the tumor board, the operating surgeon confirmed that the lesion was indeed a large intranasal polyp, easily shelled out during resection and removed intact en-bloc after stalk ligation. The clinical impression was that the stalk originated from the medial wall of the maxillary antrum. Our interventional radiologist noted on embolization that the polyp was vascularized from a single contributing branch of the arteria sphenopalatina in the area of the maxillary sinus. This additional clinical information obtained at the tumor board was very helpful in establishing the final diagnosis.

Due to their anatomical structure, ACPs are prone to vascular compromise at several sites, leading to ischemia, infarction, thrombosis, and subsequent neovascularization. These changes can result in a diagnosis of "angiomatous" ACPs. While such vascular proliferations and stromal atypia can mimic soft tissue sarcomas, they likely represent reactive changes.

Differential Diagnoses (clinical and pathological)

- Tornwaldt's cysts
- Nasal glioma
- Mucocele
- Inflammatory sinonasal polyps
- Sinonasal angiofibroma
- Inverted papilloma
- Inflammatory myofibroblastic tumor
- Nasopharyngeal carcinoma
- Sinonasal hemangioma lobular capillary hemangioma
- Sinonasal angiosarcoma
- Rhabdomyosarcoma
- Lymphomas

ACPs should be distinguished from neoplasms such as sinonasal capillary or cavernous hemangiomas, which present with nasal obstruction and epistaxis and are not specific to any age or sex. Sinonasal hemangiomas preferentially occur in the anterior nasal septum (Little or Kiesselbach area; 60%), nasal vestibule, turbinate (tip), and rarely in the sinuses. Hemangiomas typically have an infiltrative border, unlike the polypoid configuration of ACPs. Hemangiomas are composed of a circumscribed, lobular arrangement of endothelial-lined capillaries. Lumina can be absent, slit-like, or prominent. They may show branching lumina. The sometimes irregular vascular channels are lined by benign-appearing, usually plump endothelial cells embedded in edematous stroma. Bland nuclei are surrounded by eosinophilic cytoplasm. There is an intimate association of spindled SMA-positive pericytes within perivascular spaces. The surrounding stroma is fibromyxoid to edematous but may be hyalinised, especially with chronicity. Mixed inflammatory cells and extravasated erythrocytes are usually present. An inflammatory component with small lymphocytes, plasma cells, mast cells, and neutrophils can usually be seen. Furthermore, ASCs should be absent, and extensive fibrosis and hemosiderin deposition would not be expected in a sinonasal hemangioma. Clonal deletion (21)(q21.2q22.12) is reported in some sinonasal hemangiomas in line with expected neoplastic clonal origin.

The continuous presence of an SMA-positive pericyte layer can be a valuable tool in differentiating between hemangiomas and angiosarcomas, but it is not without its uncertainties. Hemangiomas, particularly types like infantile and congenital hemangiomas, consistently show a well-preserved pericyte layer. This layer, highlighted by smooth muscle actin (SMA) staining, surrounds the capillaries and vessels and helps maintain vascular structure. This is a distinguishing feature of hemangiomas that are typically benign, self-limiting, and well-organized with a lobular architecture and peripheral vascular maturation. In contrast, angiosarcomas are malignant endothelial tumors known for their aggressive and poorly organized vascular architecture. Typically, these tumors display a disrupted or absent pericyte layer, making SMA staining less pronounced. The lack of a continuous SMA-positive layer often correlates with the invasive and chaotic growth patterns seen in angiosarcomas. However, some reports have documented cases of dermal and breast low-grade angiosarcomas and radiation-

induced angiosarcomas that partly retain a pericytic layer, thus blurring this distinction. This overlap can lead to diagnostic challenges, especially in cases with less aggressive angiosarcomas that preserve some vascular structure. Given this, while the presence of a continuous SMA-positive pericyte layer can help rule in a diagnosis of hemangioma, its absence does not definitively indicate malignancy, nor does its presence completely rule out low-grade angiosarcoma. The histological context, including the architecture and degree of vascular atypia, is essential for a definitive diagnosis. Therefore, while useful, the SMA-positive pericyte layer is just one piece of a larger diagnostic puzzle. Pathologists must be cautious, especially in cases where the lesion exhibits both benign and malignant features.

Angiosarcomas furthermore generally demonstrate infiltrative growth, significant necrosis, hemorrhage, and prominent endothelial atypia—features not present in this case.

Feature	**Antrochoanal Polyps**	**Hemangiomas**	**Low-Grade Angiosarcomas**
Architecture	Disorganized, infiltrative, mixed fibrous stroma and vessels	Well-defined, organized, dilated vessels	Infiltrative, complex vascular architecture
Endothelial Cell Morphology	Normal, no atypia	Normal, no atypia	Atypical, irregular nuclei, increased mitotic activity
Vascular Spaces	Dilated but uniform, no significant atypia	Uniformly dilated, may show hyaline changes	Heterogeneous, may show hemorrhage and necrosis
Patient Presentation	Common in adolescents and young adults but occur at all ages	Growing mass, can occur at any age	More aggressive symptoms, possible pain and ulceration

Feature	Antrochoanal Polyps	Hemangiomas	Low-Grade Angiosarcomas
Imaging Studies	Well-defined mass, often from maxillary sinus. Bone remodelling occur.	Well-circumscribed vascular lesion	Infiltrative destructive mass with irregular borders
Immunohistochemistry	Positive for endothelial markers, normal p53/Ki-67 expression	Positive for endothelial markers, normal p53/Ki-67 expression	Strong positivity for endothelial markers, aberrant p53/Ki-67 expression

In our patient, the clinical and radiological presentation suggested an aggressive malignant tumor, and the results of several preoperative biopsies were inconclusive, raising the possibility of vascular neoplasms, including hemangioma and angiosarcoma. The striking vascular proliferation and ectasia associated with amorphous eosinophilic material present in biopsy and resection specimens were, in retrospective evaluation at the multidisciplinary conference, in my view more consistent with an ACP. Despite the preoperative concerns for malignancy, it became evident at surgery that the tumor was a benign and easily excisable polyp originating in the maxillary antrum. Additionally, bleeding was minimal both during and after surgery.

It is important that a correct diagnosis of these lesions be made, as they require different treatments and carry different prognoses. ACP's share the benign clinical characteristics of all inflammatory sinonasal polyps, i.e., excision is curative and recurrences are rare. This contrast with hemangiomas, angiosarcomas, and other neoplastic differential diagnoses, which require either complete surgical excision and/or radiotherapy to prevent recurrence.

One last remark is that sometimes polyps do have a core of neoplastic tissue that drive the polyp formation. I am thinking of things like a skin fibroepithelial polyp where we occasionally find a nevus at the tip or the rare giant fibrovascular polyp in the upper aerodigestive tract where most cases now are believed to be secondary to atypical lipomatous tumors (ALT/WD lipoma like LPS). Still the pathogenesis of ACP is rather speculative so perhaps good to keep an open mind.

Conclusions

- Angiomatous ACP is a rare subtype of inflammatory sinonasal polyp characterized by excessive vascular proliferation and stromal cell atypia, which can pose diagnostic challenges.
- ACPs can occur across a wide age spectrum, although they are more common in younger populations.
- Imaging findings may suggest malignancy due to bone remodeling.
- Biopsies are often inconclusive.
- Key diagnostic features include lobular growth, mild endothelial and stromal cell atypia, low proliferation rates, and a continuous pericyte layer.
- Clinical peroperative identification of a polyp stalk originating from the maxillary sinus is crucial for accurate diagnosis.
- Subspecialized sign-out is generally preferred, but if specimens end up on the wrong speciality desk, diagnoses can be challenging.
- If one is not aware of a diagnostic entity it is difficult to make the correct diagnosis.
- Reading about relevant differential diagnoses is a valuable practice.
- Intercollegial consultation and multidisciplinary team discussions at tumor boards can aid in resolving diagnostic challenges.

References

1. Ruysch, F. (1691). *Observationum Anatomica-Chirurgicarum Anturca*.
2. Zuckerkandl, E. (1892). *Normale und pathologische Anatomie der Nasenholme*. Vienna.
3. Killian, G. (1906). The origin of choanal polypi. *Lancet*, 2, 81-82.
4. Batsakis, J. G., & Sneige, N. (1992). Choanal and angiomatous polyps of the sinonasal tract. *Annals of Otology, Rhinology & Laryngology*, 101, 623-625.
5. Yfantis, H. G., et al. (2000). Angiectatic nasal polyps that clinically simulate a malignant process: Report of two cases and review of the literature. *Archives of Pathology & Laboratory Medicine*, 124, 406-410.
6. Crotty, S. P., et al. (2005). Infarcted angiomatous nasal polyps. *European Archives of Oto-Rhino-Laryngology*, 262, 225-230.
7. Frosini, P., et al. (2009). Antrochoanal polyp: Analysis of 200 cases. *Acta Otorhinolaryngologica Italica*, 29, 21-26.
8. Kumar, B., et al. (2012). Infarcted angiectatic nasal polyp with bone erosion and pterygopalatine fossa involvement—simulating malignancy: Case report and review of the literature. *The Internet Journal of Pathology*, 13(2), 1-5.
9. Jayaram, S., et al. (2014). Angiectatic nasal polyp – the great imitator. *The Internet Journal of Otorhinolaryngology*, 15(1), 1-3.
10. Tam, Y., et al. (2016). The clinicopathological features of sinonasal angiomatous polyps. *International Journal of General Medicine*, 9, 207-212.
11. Choudhury, N., et al. (2018). Diagnostic challenges of antrochoanal polyps: A review of sixty-one cases. *Clinical Otolaryngology*, 43(2), 670-674.
12. Mitteldorf, C., et al. (2018). Deceptively bland cutaneous angiosarcoma on the nose mimicking hemangioma: A clinicopathologic and immunohistochemical analysis. *Journal of Cutaneous Pathology*, 45, 652-658.

13. Mandal, S., et al. (2019). Osseous metaplasia of antrochoanal polyp: Case report and radiological-pathological correlation. *Indian Journal of Radiology and Imaging*, 29, 468-471.
14. Neena, C., et al. (2019). Massive angiomatous nasal polyp mimicking nasopharyngeal angiofibroma. *Indian Journal of Otolaryngology and Head and Neck Surgery*, 71 Suppl. 2, 2114-2116.
15. Guntur, S., et al. (2019). Rare case of an angiectatic sinonasal polyp feigning malignancy. *Journal of Cancer Research and Therapeutics*, 15, 733-736.
16. Purushothaman, P. K., et al. (2020). Angiectatic sinonasal polyp: A diagnostic challenge. *Indian Journal of Otolaryngology and Head and Neck Surgery*, 73, 260-262.
17. Assiri, K. S., et al. (2020). Clinical and pathological features of angiomatous nasal polyps: A report of four cases and review of the literature. *Cureus*, 12, e7642.
18. Warman, M., et al. (2021). Inflammatory profile of antrochoanal polyps in the Caucasian population – a histologic study. *American Journal of Rhinology & Allergy*, 5(5), 664-673.
19. Zhao, X., et al. (2023). Angiectatic nasal polyps with pleomorphism—a diagnostic pitfall. *Brazilian Journal of Otorhinolaryngology*, 89(4), 1-7.
20. Gervais, M.-K., et al. (2017). Clinical outcomes in breast angiosarcoma patients: A rare tumor with unique challenges. *Journal of Surgical Oncology*, 116, 1056–1061.
21. Zhang, H., et al. (2021). Vascular lesions of the breast: Essential pathologic features and diagnostic pitfalls. *Human Pathology Reports*, 26, 1-7.

AMR SEMINAR #80
Ca se 8

Case contributed by: Brandon Larsen, M.D., Ph.D., Mayo Clinic, Scottsdale, AZ.

Clinical History: A 66-year-old man and former smoker was found to have scattered bilateral pulmonary nodules on a lung cancer CT screening study. He has no prior history of malignancy or immunosuppression. He is a retired Iraqi airforce pilot and moved to the United States from Iraq in 1998. He continues to visit Iraq on a yearly basis. Because of a high clinical concern for malignancy, two of the lung nodules were resected for a definitive diagnosis and to obtain material for molecular testing. A section of one of these nodules is provided here, which represents both resected lesions.

Pathology: The resected lung tissue shows a nodular granulomatous fibroinflammatory process with central necrosis that includes abundant degenerating eosinophils. Closer examination reveals a degenerating parasitic helminth within the nodule with a thick translucent laminated wall or membrane, in a pattern characteristic of *Echinococcus*. It is difficult to be absolutely certain of the species of *Echinococcus* that this represents using this material as brood capsules and protoscolices are not present, but the clinical presentation with cystic necrotic nodules is most in keeping with *Echinococcus granulosus*. No evidence of a neoplasm is seen.

Diagnosis: Pulmonary echinococcosis (hydatidosis).

Comment: Carnivorous predators (especially dogs and wolves) represent the primary hosts for *Echinococcus*, with sheep, cows, and other mammals representing its natural intermediate hosts. The adult *Echinococcus* lives in the intestines of infected canids and its eggs are shed in feces and ingested by the intermediate host, where larvae develop in hydatid cysts in the liver, lungs, brain, and other organs. When the dog, wolf, or other predator eats meat containing hydatid cysts of an infected animal, the cycle repeats. Humans can also be infected through inadvertent contact, often in areas where sheep or cows are raised and slaughtered in close proximity to dogs that feed on their entrails. Humans represent a dead end in the life cycle of *Echinococcus*.

Although very rare in the United States, echinococcosis is a significant endemic public health problem in other parts of the world, especially the Middle East, East Africa, Central Asia, parts of China, and some parts of South America. Infections can go undetected for many years or decades. In this patient, the source of his infection was unknown, but he was probably exposed while living or traveling in Iraq, perhaps even in his childhood.

I found this to be a quite lovely example of this problem that is only rarely encountered in surgical pathology practice in wealthy industrialized nations and thought the AMR Club would appreciate seeing it as well. It is not a difficult diagnostic problem but is probably still worth reviewing given its rarity for most of us. I hope you enjoy it.

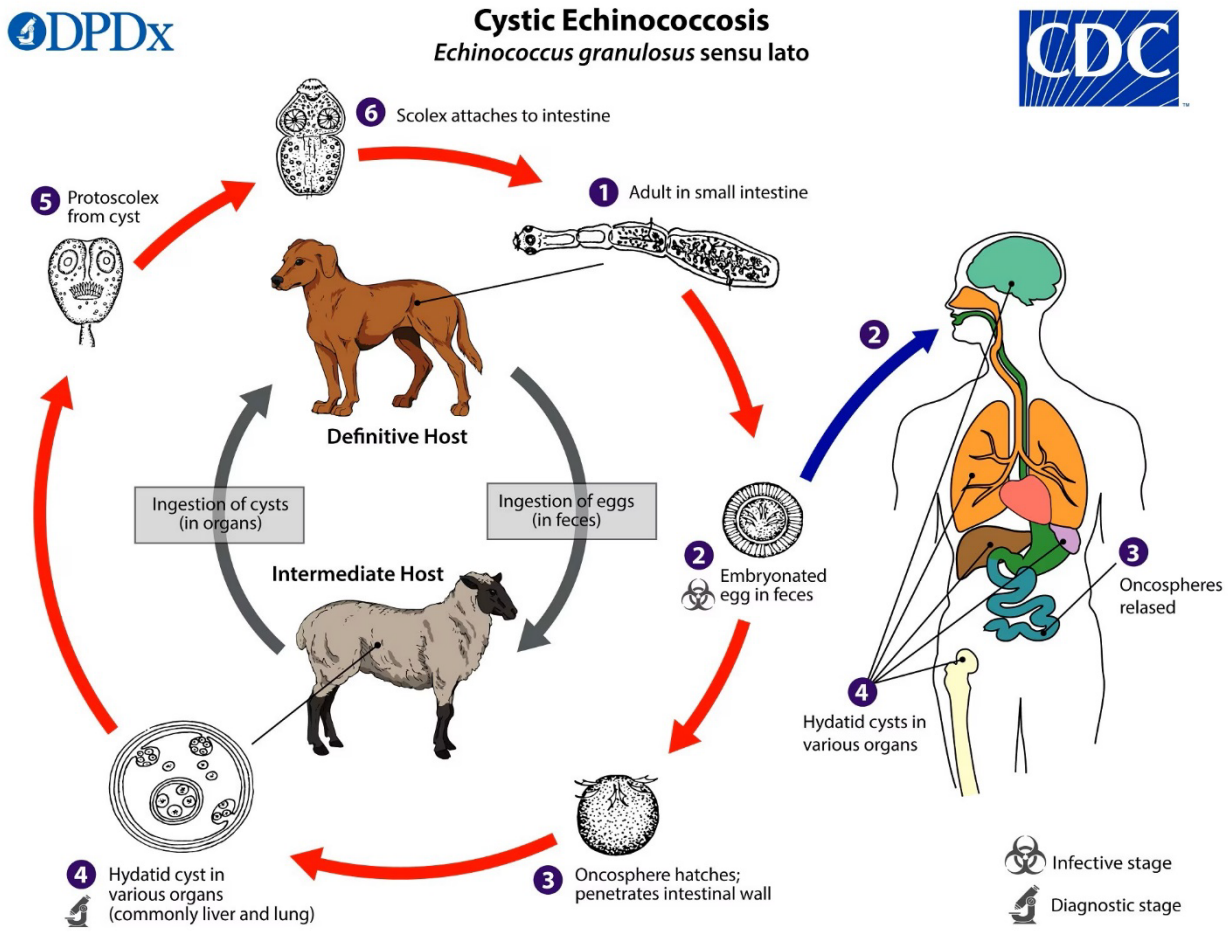

References:

1. Echinococcosis. Department of Laboratory Identification of Parasites of Public Health Concern, United States Centers for Disease Control and Prevention; cdc.gov/dpdx/echinococcosis/index.html. Accessed Jan. 9, 2025
2. Morar R, Feldman C. Pulmonary echinococcosis. *Eur Respir J*. 2003;21:1069-77.
3. Aytac Y, Yurdakul C, Ikizler C, et al. Pulmonary hydatid disease: report of 100 patients. *Ann Thorac Surg*. 1977;23:145-51.

AMR SEMINAR #80
Ca se 9

Case contributed by: Jesse Mackinney, M.D., Cleveland Clinic, USA.

Clinical history: The patient is 47-year-old man with a 6.2 cm right renal mass.

Pathologic findings: This tumor shows a spectrum of histologic features described in classic papillary RCC, as defined by the current WHO (i.e. the historical “type 1” group). However, instead of a single large, encapsulated cyst filled with papillary structures, this tumor is characterized by numerous smaller encysted aggregates separated by fibrous stroma. In addition, there is spread into extrarenal adipose tissue.

Diagnosis: Papillary renal cell carcinoma, WHO/ISUP Grade 3 with microcystic features.

Discussion: Prognostic stratification in renal cell carcinoma has evolved significantly over the past decade, largely driven by the description of new subtypes. Papillary RCC is now more homogeneous because other distinct aggressive tumors (previously regarded as “type 2” papillary RCC) are now regarded as separate “entities” (e.g. FH-deficient RCC, acquired cystic disease-associated RCC, TFE3 rearranged RCC, TFEB rearranged RCC, TFEB amplified RCC, etc). Therefore, it is now easier to attempt prognostic stratification studies in this more restrictive group of papillary RCC.

Sarcomatoid differentiation and (rarely) poorly differentiated/anaplastic transformation explain many of the aggressive outcomes in this group, but not all papillary RCC with metastatic disease have these two frankly aggressive histologic patterns. There have been several studies suggesting that architectural patterns may be more prognostic than nuclear grading as 1, 2, or 3. Specifically, an initial study looked at solid, hobnail, and micropapillary histology, which they described as “unfavorable architecture.” In our experience, these unfavorable architectural features co-vary with the low power “microcystic architecture” demonstrated by this current case, characterized by numerous epithelial-lined cysts containing the papillary tumor and separated by fibrous stroma. Our data suggest this pattern is a more specific predictor of metastatic potential and is more reproducible. We hope that other groups will study these patterns, particularly controlling for each histologic pattern and pathologic stage.

References:

1. Yang C, Shuch B, Kluger H, Humphrey PA, Adeniran AJ. High WHO/ISUP Grade and Unfavorable Architecture, Rather Than Typing of Papillary Renal Cell Carcinoma, May Be Associated with Worse Prognosis. *Am J Surg Pathol* 2020;44(5):582-593. PMID: 32101890.

2. Chan E, Stohr BA, Butler RS, Cox RM, Myles JL, Nguyen JK, Przybycin CG, Reynolds JP, Williamson SR, McKenney JK. Papillary Renal Cell Carcinoma with Microcystic Architecture Is

Strongly Associated with Extrarenal Invasion and Metastatic Disease. *Am J Surg Pathol* 2022;46(3):392-403. PMID: 34881751.

3. Zhao T, Denize T, Wang H, Fisch AS, Wu S, Wu CL, Cornejo KM. Multinucleated tumor cells and micropapillary morphology appear to be predictors of poor prognosis in renal cell carcinoma with papillary and oncocytic features. *Hum Pathol* 2024;153:105677. (Epub ahead of print) PMID: 39489385.

AMR SEMINAR #80
Ca se 10

Case contributed by: Anais Malpica, M.D. Anderson Cancer Center, USA.

Clinical History: A 29 year-old female presented with a history of heavy vaginal bleeding for 4 months requiring transfusion of red blood packed cells and iron transfusion. An endometrial biopsy was obtained and interpreted as endometrial hyperplasia without atypia. The patient was given treatment with high dose progesterone which she did not tolerate. Then, she underwent dilatation and endometrial curettage as well as the insertion of Mirena IUD. The endometrial curettage was initially interpreted as atypical endometrial hyperplasia. The patient requested a second opinion regarding her management and the over read of her endometrial curetting was endometrial mesonephric-like carcinoma. Subsequently, the patient underwent a robotically assisted, laparoscopic hysterectomy with bilateral salpingo-oophorectomy, sentinel lymph node sampling and omental sampling. The patient is currently receiving whole pelvic radiotherapy and chemotherapy.

Pathologic findings: The endometrial tumor measured 4.0 x 2.3 x 1.5 cm and invaded into the outer half of the myometrium. The tumor is composed of glands, some of them with papillary structures, tubules and focal solid areas. The neoplastic cells are either columnar or cuboidal with scattered hobnail cells. The cytoplasm is mostly amphophilic and focally eosinophilic. The nuclear:cytoplasmic ratio is increased, there is some nuclear overlapping, and there are 3 mitoses per 10 HPFs. The nuclei show chromatin clearing, some grooves and a few visible nucleoli. Focally, the presence of intraluminal eosinophilic contents is noted.

Immunohistochemical studies show that the tumor cells were diffusely positive for TTF-1, patchy positive for GATA-3 and negative for ER and PR. The expression of p53 was wild type and the nuclear expression of MLH1, PMS2, MSH2 and MSH6 was retained

Diagnosis: Mesonephric-like carcinoma of uterus.

Note: the tumor invaded 57% of the myometrial wall and showed vascular lymphatic invasion. Macrometastasis were noted in 2/6 right obturator sentinel lymph nodes and isolated tumor cells were seen in 2/10 left obturator sentinel lymph nodes. The uterine cervix, bilateral adnexa, and omentum were free of tumor.

Discussion: Mesonephric-like carcinoma is an uncommon tumor seen in women with a wide age range, 28-91 years, who typically present with uterine bleeding. It usually arises in the endometrium, and occasionally occurs in the myometrium. According to the molecular classification for endometrial carcinoma, this tumor typically belongs to the NSPM (non-specific molecular profile) category; however, this is an aggressive tumor with a tendency to present at advance stage and to give metastasis to distant sites (ie, lungs, liver, bone, brain). A rare case has

shown MLH1 and PMS2 loss. Histologically, it has a wide range of architectural patterns: tubular, ductal/glandular, papillary, retiform, glomeruloid, solid, and trabecular. The cells show the features described above. In addition, spindle cells and corded formations in a hyalinized background (corded and hyalinized pattern) can be seen. Rare cases can show squamous or mucinous differentiation -including the presence of goblet cells, or be associated with atypical endometrial hyperplasia, low grade endometrioid carcinoma, carcinosarcoma or undifferentiated carcinoma.The presence of eosinophilic intraluminal contents is variable. The immunohistochemical profile typically shows TTF-1 and/or GATA-3 positivity, CD10 luminal expression, and focally positive calretinin as well as the lack of expression of ER and PR. Occasionally, some expression of ER (<10%) can be seen. PAX-8 is expressed in this type of tumor while the expression of SOX-17 is either negative or just focally positive. From the molecular standpoint, this tumor shows *Kras* mutation which can be associated with mutations in the following genes: *PIK3CA, PTEN*, and *CTNNB1*.

References:

1. Euscher ED, Bassett R, Duose DY, Lan C, Wistuba I, Ramondetta L, Ramalingam P, Malpica A. Mesonephric-like Carcinoma of the Endometrium: A Subset of Endometrial Carcinoma With an Aggressive Behavior. Am J Surg Pathol. 2020 Apr;44(4):429-443. doi: 10.1097/PAS.0000000000001401. PMID: 31725471.
2. Patel V, Kipp B, Schoolmeester JK. Corded and hyalinized mesonephric-like adenocarcinoma of the uterine corpus: report of a case mimicking endometrioid carcinoma. Hum Pathol. 2019 Apr;86:243-248. doi: 10.1016/j.humpath.2018.08.018. Epub 2018 Aug 30. PMID: 30172914.
3. Tahir M, Xing D, Ding Q, Wang Y, Singh K, Suarez AA, Parwani A, Li Z. Identifying mesonephric-like adenocarcinoma of the endometrium by combining SOX17 and PAX8 immunohistochemistry. Histopathology. 2025 Jan;86(2):268-277. doi: 10.1111/his.15312. Epub 2024 Sep 4. PMID: 39233315; PMCID: PMC11649513.
4. Mirkovic J, Olkhov-Mitsel E, Amemiya Y, Al-Hussaini M, Nofech-Mozes S, Djordjevic B, Kupets R, Seth A, McCluggage WG. Mesonephric-like adenocarcinoma of the female genital tract: novel observations and detailed molecular characterization of mixed tumours and mesonephric-like carcinosarcomas. Histopathology. 2023 Jun;82(7):978-990. doi: 10.1111/his.14892. Epub 2023 Mar 31. PMID: 36860193..
5. Kolin DL, Costigan DC, Dong F, Nucci MR, Howitt BE. A Combined Morphologic and Molecular Approach to Retrospectively Identify KRAS-Mutated Mesonephric-like Adenocarcinomas of the Endometrium. Am J Surg Pathol. 2019 Mar;43(3):389-398. doi: 10.1097/PAS.0000000000001193. PMID: 30489318.
6. Angelico G, Salvatorelli L, Tinnirello G, Santoro A, Zannoni GF, Puzzo L, Magro G. The first evidence of mismatch repair deficiency in mesonephric-like adenocarcinoma of the endometrium: clinicopathological and molecular features of a case emphasising a possible endometrioid carcinogenesis. Histopathology. 2024 May;84(6):1068-1070. doi: 10.1111/his.15136. Epub 2024 Jan 3. PMID: 38173293.

7. Quddus MR, Mathews CA, Singh K. Ever Expanding Morphologic Patterns of Mesonephric-like Adenocarcinomas of the Uterine Corpus: A Report of Two Tumors and a Brief Review of the Literature. Int J Surg Pathol. 2024 Oct;32(7):1398-1403. doi: 10.1177/10668969241228285. Epub 2024 Feb 4. PMID: 38311895.
8. Pors J, Segura S, Chiu DS, Almadani N, Ren H, Fix DJ, Howitt BE, Kolin D, McCluggage WG, Mirkovic J, Gilks B, Park KJ, Hoang L. Clinicopathologic Characteristics of Mesonephric Adenocarcinomas and Mesonephric-like Adenocarcinomas in the Gynecologic Tract: A Multi-institutional Study. Am J Surg Pathol. 2021 Apr 1;45(4):498-506. doi: 10.1097/PAS.0000000000001612. PMID: 33165093; PMCID: PMC7954854.

AMR SEMINAR #80
Ca se 11

Case submitted by: Kyle Perry, M.D., University of Michigan, USA.

Clinical History: A young adult patient complained of a raised enlarging and erythematous nodule in the skin of the right mandible. Clinically, this measured 3.0 x 3.0 cm in size. On gross examination, the lesion appeared to measure 1.8 cm in greatest dimension.

The sections show a vascular neoplasm that appears to be centered in the dermis and is intimately associated with cutaneous adnexal structures (Figure 1A). On higher power examination, there are prominent dilated spaces reminiscent of a venous hemangioma (Figure 1B). Other areas of the tumor, however, exhibited a more retiform architecture adjacent to endothelial cells with a vague spindled appearance (Figure 1C). Still other areas of the lesion were characterized by solid aggregates of endothelial cells, some of which exhibited cytoplasmic vacuolization (Figure 1D).

The cells were diffusely positive for CD31 (Figure 2A) and negative for CD34 (Figure 2B). The cells exhibited diffuse expression for synaptophysin (Figure 2C) and showed almost no expression of CD56 (Figure 2D). The cells were positive for ERG and were negative for CAMTA1, HHV8 and chromogranin.

Diagnosis: Composite hemangioendothelioma with neuroendocrine marker expression

Comments: I thought that this was a very nice example of a composite hemangioendothelioma with neuroendocrine marker expression. Dr. Andrew Folpe recognized this group of composite hemangioendotheliomas which exhibited a heterologous but reproducible morphology composed of retiform hemangioendothelioma-like vascular channels, more solid arrangements of epithelioid-like endothelial cells reminiscent of epithelioid hemangioendothelioma and hemangioma-like areas composed of dilated vascular spaces. CHE with neuroendocrine expression has been reported in both superficial and deep anatomic sites.

Immunohistochemistry showed these tumors to be consistently positive for CD31, ERG and FLI1 while only about half stained for CD34. They are negative for CAMTA1. Synaptophysin was consistently expressed in the endothelial cells in these tumors while CD56 was only present half the time. Chromogranin expression was not typically seen.

CHE with neuroendocrine marker expression has been found to exhibit *PTBP1::MAML2* in 5 cases while one case was found to exhibit *EPC1::PHC2* fusion.

While the behavior of composite hemangioendothelioma is generally acknowledged to be less aggressive than angiosarcoma, neuroendocrine composite hemangioendothelioma is thought to

behave more aggressively with distant metastasis reported in approximately half of patients. (1-3)

Special thanks to Dr. Paul Harms for allowing me to share this case.

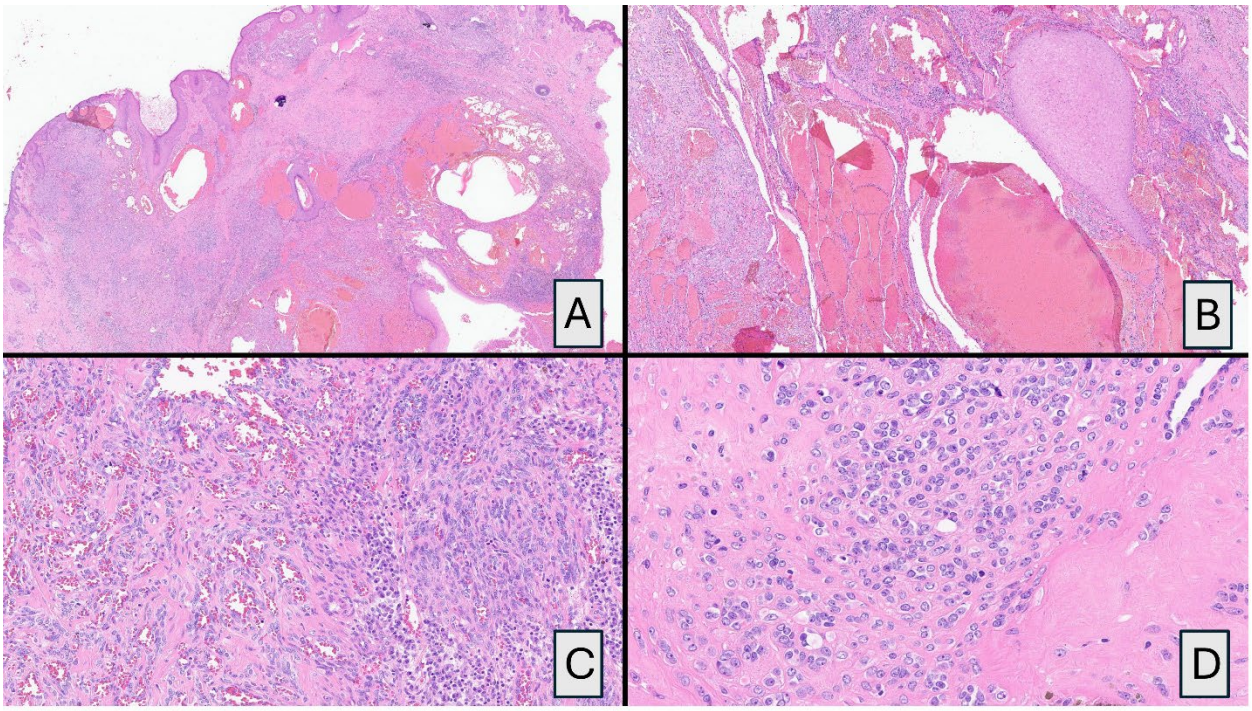

Figure 1: Composite hemangioendothelioma presenting as a superficial mass (A). Many areas of tumor exhibited features of a hemangioma (B). Others showed a distinct retiform architecture adjacent to spindled endothelial cells (C). Other areas of the tumor exhibited cytoplasmic vacuolization, reminiscent of epithelioid hemangioendothelioma (D).

AMR SEMINAR #80
Ca se 12

Case contributed by: Fred Petersson, M.D., University of Singapore, Malaysia.

Case history: The patient is a 70-year-old male with history of sigmoid adenocarcinoma (status-post anterior resection and adjuvant chemotherapy), who presented with a painless lump at the tongue/right floor of mouth with a duration of two years. He was not known to have tuberous sclerosis. On clinical examination, there was a 4.0×3.0 cm soft, sessile, mucosa-covered swelling on the right FOM that did not cross the midline.

Gross findings: Intraoperatively a 7.0×3.0 cm reddish-brown tumour arising from either the right genioglossus or hyoglossus muscle was identified. The tumour was well-demarcated from the surrounding musculature/tissues and easily enucleated. At gross examination, the tumour was received as a reddish-brown, lobulated, fleshy, and slightly friable mass.

Histological findings + IHC: On light microscopic examination, the tumour was multilobulated and unencapsulated. The tumour consisted of diffuse sheets of polygonal cells, with abundant optically clear cytoplasm. The polygonal cells varied markedly in size—with some showing voluminous cytoplasm. These clear cells had small, peripherally displaced pyknotic, hyperchromatic nuclei, compressed against the inner aspect of the cell membranes. The cell membranes were distinct and very well defined, somewhat reminiscent of the cell walls of vegetable material/plant cells. In some of the clear cells, there was wispy eosinophilic material within the cytoplasm. Ample periodic acid-Schiff (PAS) positive (diastase sensitive) material consistent with glycogen in the clear cytoplasm was identified. Admixed with the sheets of clear cells were polygonal cells with eosinophilic granular cytoplasm, which accounted for approximately 20% of tumour cell composition/mass. In contrast to the clear cells, the cells with eosinophilic cytoplasm had centrally placed nuclei with less condensed chromatin and frequently small but distinct nucleoli. At high magnification, focal features of skeletal muscle differentiation (cross striations) and intracytoplasmic crystalline material were present. These features were better appreciated on a PTAH- stained section. Some of the cells with skeletal muscle differentiation displayed multivacuolated cytoplasm with retraction of the cytoplasm from the cell wall, forming spindly attachments resembling spider webs (corresponding to the classical “spider” cells). No mitotic activity or necrosis was identified. On immunohistochemistry, the tumour cells were positive for desmin, with focal myogenin- and myoD1- expression. Focal expression of SMA was present. The cells showed no expression of cytokeratins (AE1/3 and Cam5.2), p63, PAX8, S-100 protein, SOX10, CD68 and CD163. Interestingly, desmin immunoexpression was limited to the periphery of the cytoplasm, just beneath the cell membrane in the clear cells, while diffusely and strongly positive in the cells with eosinophilic cytoplasm—imparting a “checkerboard” appearance.

Diagnosis: Adult rhabdomyoma, clear cell variant**.**

Comments: This is not a spectacular case, especially not for my superb soft tissue specialized colleagues in the club, but I still think the case could be appreciated by the members. For those who are interested in a more in-depth information about this topic/case, it was just recently published [1]. Awareness of the fact that this uncommon tumour may uncommonly acquire extensive clear cell-change is important for people signing out H&N cases, since in the H&N region a clear cell tumour, raises several diagnostic possibilities. This is especially true on a core- or FNA-biopsy sample where the predominant clear cell component is likely to be preferentially sampled.

Clear cell change in other soft tissue tumours exhibiting muscle differentiation has been previously reported. These include clear cell rhabdomyosarcoma of the pharynx [2] and uterine epithelioid leiomyosarcomas with clear cells [3]. In ccRMS, clear cell change has been attributed to accumulation of intracytoplasmic glycogen. The presence of increased mitotic activity, necrosis and frankly infiltrative growth are readily identified features that separates ccRMS from a ccAR. From a differential diagnostic perspective, the histomorphology of clear cell AR variably overlaps with other clear cell-rich neoplasms of the H&N region. This may lead to diagnostic problems, especially on limited biopsy material and FNA-specimens. Hence awareness of that AR may display extensive clear change is thus of importance for the practicing (H&N-) pathologist. The main differential diagnostic considerations include metastatic carcinomas (renal, thyroid, parathyroid etc) and salivary gland neoplasms with extensive clear cell change/morphology. In the tongue, a clear cell variant of thyroid carcinoma arising from ectopic/extrathyroidal thyroid tissue could also be contemplated.

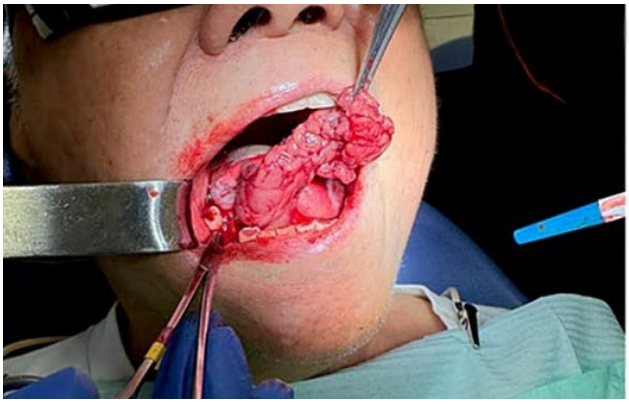

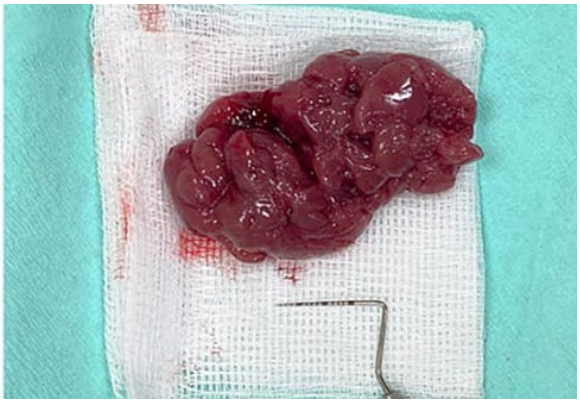

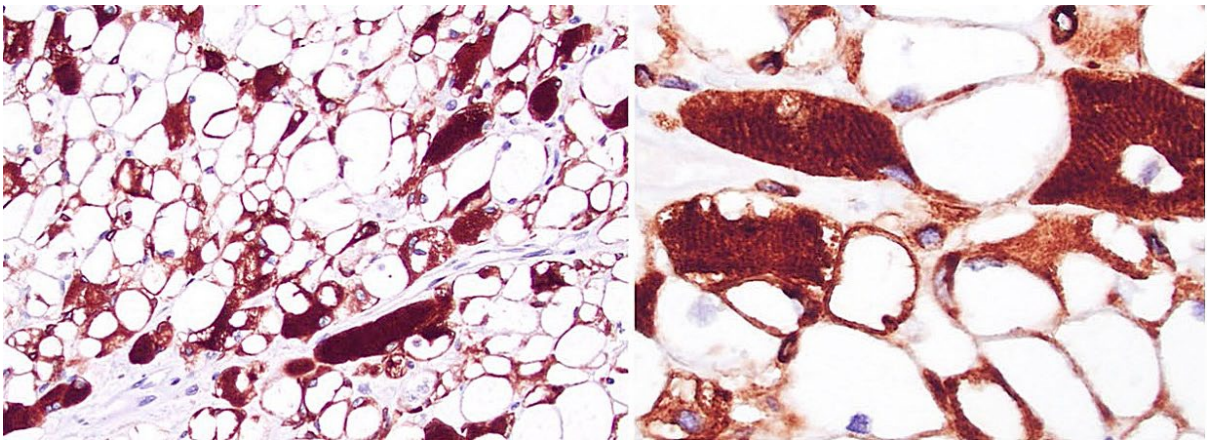

Desmin IHC.

References:

1. Clear cell adult rhabdomyoma-a rare variant of an unusual tumour. Oon ML, Wu B, Lim R, Liew MKM, Petersson F. Virchows Arch. 2024 Jun 14. doi: 10.1007/s00428-024-03850-4.

2. Boman F, Champigneulle J, Schmitt C et al Clear cell rhabdomyosarcoma. 1996 Pediatr Pathol Lab Med 16:951–959

3. Silva EG, Deavers MT, Bodurka DC, Malpica A Uterine epithelioid leiomyosarcomas with clear cells: reactivity with HMB-45 and the concept of PEComa. 2004 Am J Surg Pathol 28:244–249.

AMR SEMINAR #80
Ca se 13

Case contributed by: David Suster, M.D, Rutgers University, USA.

Clinical History: A 54-year-old male underwent a segmental resection of his small bowel for invasive adenocarcinoma. At the time of microscopic examination there was an unusual lobulated proliferation of nodules of myxoid stroma with a delicate vascular network and scattered small atrophic adipocytes that resembled small signet-ring like cells and raised concern for a signet ring cell carcinoma component as well as the possibility of a myxoid soft tissue sarcoma. Some of the cells demonstrated pigment within the cells. The cells were strongly and diffusely positive for S100 and the pigment stained positive with iron. Immunostains for cytokeratin AE1/AE3, CK7, BerEP4, HMB45, Melan A and MDM2 were negative. FISH for DDIT3 was performed and was negative.

Diagnosis: Pseudoneoplastic fat atrophy.

Discussion: Pseudoneoplastic fat atrophy is an unusual reactive change that may be confused for tumoral conditions. Patients undergoing periods of starvation or malnutrition may develop degenerative and/or atrophic changes of various organs. These findings may manifest histologically, particularly in areas of adipocytic tissue, and may cause confusion when first encountered, raising a differential that includes benign and malignant tumor entities. Cases of this reactive process are sometimes sent in consultation to exclude signet ring cell carcinoma, liposarcoma and other tumor types. The finding appears to be linked to nutritional deficiency and is almost always associated with cachexia. Histologically, the lesions demonstrated lobules of atrophic-appearing fat with small signet-ring adipocytes that are sometimes bilobed (**Figure 1**). The nodules varied in size and were characterized by a variably myxoid stromal background, often with a prominent delicate capillary network. Fat atrophy in the peri-intestinal fat of cachectic patients can mimic signet ring cell adenocarcinoma or mesenchymal neoplasms. Nomenclature to describe this phenomenon has been inconsistent in the literature; we suggest “pseudoneoplastic fat atrophy.” Knowledge of this finding can help prevent an incorrect diagnosis and limit unnecessary ancillary testing. We have recently studied this phenomenon (yet unpublished) in a series of 10 patients (Table 1). Of note, the main importance of recognizing this phenomenon is to prevent confusing it with a diagnosis of neoplasia and importantly, also to prevent over-testing.

Figure 1: Histologic features of pseudoneoplastic fat atrophy demonstrating nodules of atrophic fat with myxoid stromal changes. The areas are positive for S100 and negative for cytokeratin.

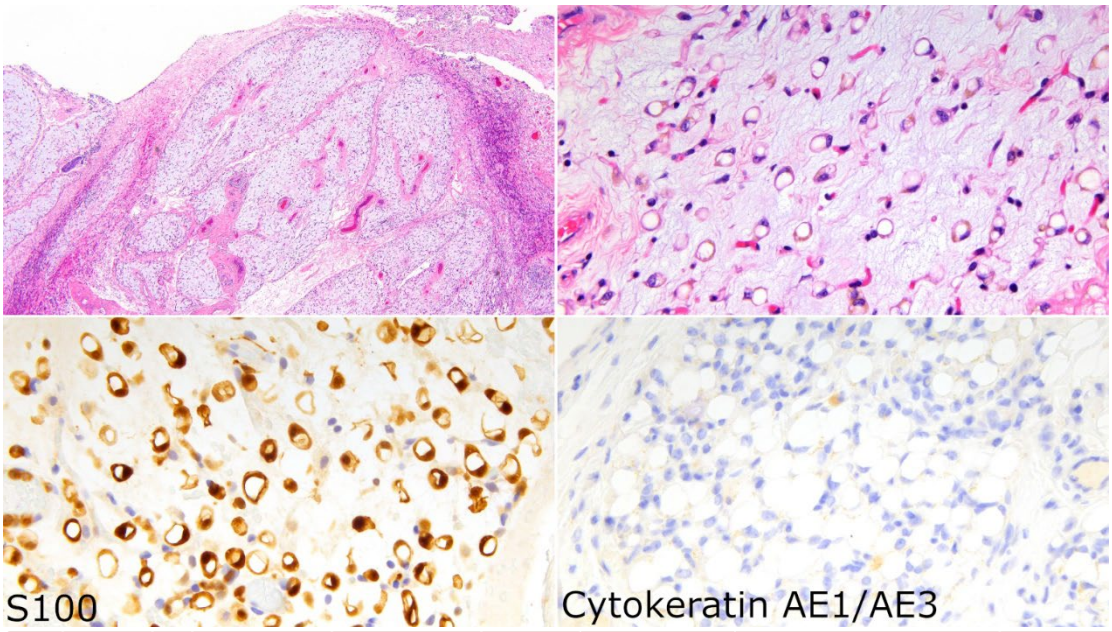

Case #	Age (years)	Sex	Cachexia	Relevant Past Medical History	Location	Procedure	Diagnostic testing	Suggested diagnoses
1	76	F	Yes		Sigmoid colon	Segmental resection	Positive: S100 Negative: ERG, CDX2, PAX8, GATA3, Cytokeratin AE1/AE3, SOX10, CD68	- Degenerative changes - Signet ring cell adenocarcinoma - Liposarcoma - Mesothelioma - Vascular lesion
2	66	F	Yes		Small intestine	Segmental resection	Positive: S100 Negative: Pancytokeratin, MDM2, calretinin, CD68, ERG, CDX2, KIT, CD1a	- Dystrophic mesenteric adipocytes
3	60	F	Yes	C. difficile colitis	Colon	Segmental resection	Positive: S100 Negative: Pancytokeratin, CD68, ERG, CD31, HMB45	- Subserosal fat degeneration with signet ring-shaped lipocytes
4	29	M	No (eventual severe malnutrition)	Colorectal adenocarcinoma	Colon	Segmental resection	Not performed	- None (finding noted, but not reported)
5	54	M	Yes		Small intestine	Segmental resection	Positive: S100, iron stain Negative: Cytokeratin AE1/AE3, CK7, BerEP4, HMB45, Melan A, MDM2 (FISH), DDIT3 (FISH)	- Degenerative adipocytes - Liposarcoma - Myxoid liposarcoma - Signet ring cell carcinoma - Melanoma
6	74	M	N/A	Colorectal adenocarcinoma	Left colon	Segmental resection	Negative: Pancytokeratin, CD34, CD68	- Degenerative adipocytes - Signet ring cell carcinoma - Vascular lesion
7	69	M	No	Colorectal adenocarcinoma	Cecum	Right hemicolectomy	Positive: S100 Negative: Cytokeratin AE1/AE3, CD68	- Signet ring cell carcinoma - Fat atrophy
8	55	M	Yes	PEG tube-dependent with severe protein malnutrition	Abdomen (hernia sac)	Emergent sigmoid colostomy and umbilical herniorrhaphy	Positive: S100 (variably) Negative: CD34, ERG, CK7, CK20, CDX2, pancytokeratin AE1/3, CAM5.2 and CD68	- Degenerative adipocytic changes - Benign "lipoblastoma-like" proliferation
9	60	F	Yes	Unintentional weight loss (30 lbs.)	Omentum, paratubal soft tissue	Bilateral salpingo-oophorectomy and omentectomy	Positive: S100, CD10, calretinin Negative: CD34, WT1, CK7, CK20, PAX8, GATA3, HMB45, CDX2, inhibin, CK5/6, ER, PR	- Degenerative adipocytic changes - Benign "lipoblastoma-like" proliferation
10	Newborn	M	Yes		Omentum	Omentectomy	Not performed	- Reactive changes

References:

1) Zhang X, Findeis-Hosey JJ. Dystrophic Adipocytes Mimicking Metastatic Signet Ring Cell Adenocarcinoma: A Diagnostic Pitfall in a Cachectic Patient. *Case Rep Pathol*. 2018;2018:9027870. Published 2018 May 7. doi:10.1155/2018/9027870
2) Houghton O, Herron B. Benign signet ring cells in the subserosa of the small intestine: a pseudoneoplastic phenomenon. *Ulster Med J*. 2006;75(1):93-94.
3) Milan G, Murano I, Costa S, et al. Lipoatrophy induced by subcutaneous insulin infusion: ultrastructural analysis and gene expression profiling. *J Clin Endocrinol Metab*. 2010;95(7):3126-3132. doi:10.1210/jc.2009-2773

AMR SEMINAR #80
Ca se 14

Case contributed by: Daniel Wong, M.D., Nedlands, Australia.

Clinical History: 25-year-old female, previously well, with left medial knee pain and swelling. MRI showed a 7.5cm enhancing mass eroding the posterior proximal tibia, associated with marrow oedema. No mineralization on plain films. No metastatic disease on CT chest.

Macroscopic Features: Open incisional biopsy, comprising multiple pieces of soft cream-coloured tissue.

Histological, Immunohistochemical and Molecular Genetic Findings: The incisional biopsy showed a cellular tumor involving extra-osseous soft tissues and permeating bony intertrabecular spaces. There was a distinctive nested and pericytic growth pattern, with prominent epithelioid morphology. Repetitive nests, occasional larger nodules and trabeculae of epithelioid cells were present, closely associated with a rich, arborising capillary network. Scattered hyaline globules, cystic change sometimes with fibrinoid degeneration and loosely-clustered multinucleated osteoclast-type giant cells were also present. There was no convincing osteoid or cartilaginous matrix production. The tumor cells were generally monomorphic, with rounded nuclei, finely granular chromatin, small nucleoli and moderate volumes of amphophilic cytoplasm. Mitotic activity was brisk with >30 mitoses per 10 consecutive HPF. There was also focal tumour necrosis and a focus of vascular invasion.

The tumor cells show positive nuclear and cytoplasmic staining for STAT6 and GLI1, with weak focal staining for EMA. Negative markers included AE1/AE3, CAM5.2, MNF116, CD34, S100, SOX10, synaptophysin, chromogranin, melan-A, HMB45, h-caldesmon, desmin and ERG.

Interphase FISH analysis showed high-level amplification of *GLI1 / DDIT3* and *MDM2*. There was no rearrangement of *EWSR1, SS18* and *NCOA2*.

Diagnosis: *GLI1*-altered epithelioid mesenchymal neoplasm / sarcoma.

Comments: The nested and pericytic growth, epithelioid morphology and evidence of *GLI1* amplification on immunohistochemistry and FISH are consistent with the emerging entity "GLI1-altered epithelioid mesenchymal neoplasm."[1, 2] These lesions typically affect young to middle-aged adults, without gender predilection and are more commonly recognized in the head and neck but can occur at any site. The nomenclature presently avoids a malignant designation due to variable clinical behavior, although the aggressive growth on imaging, high mitotic activity and focal necrosis would suggest that the current tumor is a sarcoma. It is unclear whether the lesion is bone or soft tissue in origin, although the former is rare with only one other report in the literature to my knowledge.[3]

Central to the classification of this tumor is the genetic alteration of *GLI1* (a key regulator of the Hedgehog signalling pathway), which can be either a rearrangement or amplification (as in this case).[1, 4] This case illustrates some interesting and potentially confounding secondary immunohistochemical and molecular genetic findings related to the *GLI1* alteration. The STAT6 staining observed is presumably due to co-amplification of the *STAT6* gene which is closely situated to *GLI1* at 12q13. (However, in my experience, the staining pattern is different to that seen in solitary fibrous tumor (SFT) in showing both nuclear and cytoplasmic reactivity, similar to dedifferentiated liposarcoma and intimal sarcoma when *STAT6* is co-amplified with *MDM2*). The co-amplification of *DDIT3* and *MDM2* identified on FISH is similarly due to their proximity to *GLI1* at 12q13-15. This is the basis for the ability to use the *DDIT3* FISH probe as a surrogate marker of *GLI1*, although the co-amplification of *MDM2* can potentially mislead to a diagnosis of osteosarcoma and dedifferentiated liposarcoma in this setting (osteosarcoma was suggested on the prior core biopsy for this reason).

References:

1. Cloutier JM, Kerr DA. GLI1-Altered Mesenchymal Tumors. *Surg Pathol Clin*. 2024; 17: 13-24.
2. Antonescu CR, Agaram NP, Sung YS, et al. A Distinct Malignant Epithelioid Neoplasm With GLI1 Gene Rearrangements, Frequent S100 Protein Expression, and Metastatic Potential: Expanding the Spectrum of Pathologic Entities With ACTB/MALAT1/PTCH1-GLI1 Fusions. *Am J Surg Pathol*. 2018; 42: 553-60.
3. Kerr DA, Pinto A, Subhawong TK, et al. Pericytoma With t(7;12) and ACTB-GLI1 Fusion: Reevaluation of an Unusual Entity and its Relationship to the Spectrum of GLI1 Fusion-related Neoplasms. *Am J Surg Pathol*. 2019; 43: 1682-92.
4. Agaram NP, Zhang L, Sung YS, et al. GLI1-amplifications expand the spectrum of soft tissue neoplasms defined by GLI1 gene fusions. *Mod Pathol*. 2019; 32: 1617-26.

AMR SEMINAR #80
Quiz Case 1

Case contributed by: Volkan Adsay, M.D, Turkey.

Clinical history: This 50 years old female presented to her gynecologist with right lower quadrant abdominal pain for 3 weeks. Past history included smoking (20 pack years) and Hashimoto with thyroid replacement therapy. She does not report any prior abdominal surgery. Radiologic studies revealed a multilocular cystic lesion in the right pelvis that was also adherent to the cecal wall. The cyst appeared heterogenous and partially hemorrhagic. With the pre-operative diagnosis of primary cecal/appendiceal malignancy, the patient underwent exploratory laparoscopy with the consent of performing right hemicolectomy and HIPEC, if necessary. However, during the operation only the removal of the cystic lesion was conducted as the cyst could be shelled of from the cecal wall; and further therapy (including additional surgery, if needed) was left to the final pathologic evaluation of the cystic lesion. There were no other lesions in the abdomen.

Gross findings: A 7 x 5x 4 cm multilocular cystic partially hemorrhagic and necrotic appearing heterogenous mass located at the peri-cecal soft tissues. Appendix vermiformis was dilated with fecalith and showed mildly fibrinous surfaces.

AMR SEMINAR #80
Quiz Case 2

Case contributed by: Franco Fedeli, M.D., Florence, Italy.

Clinical History: A 47 y.o. male is seen for a paravertebral soft tissue mass that measured 7 x 4.5 x 1.7 cm. The cut surface was whitish.

AMR SEMINAR #80
Quiz Case 3

Case contributed by: Saul Suster, M.D., Rutgers University, USA.

Clinical history: A 38 year old woman had an incidentally discovered pancreatic mass during a CT scan of the abdomen for evaluation of trauma to her spine. MRCP showed a 3.4 x 3.2 cm well-demarcated tumor at the junction of the pancreatic neck and body on the right midline. A subtotal pancreatectomy and splenectomy were performed. There was no history or evidence of tumor elsewhere.